Acta Pharmacologica Sinica (2017) 38: 9–28
www.nature.com/aps

Open

Original Article

Thamnolia vermicularis extract improves learning ability in APP/PS1 transgenic mice by ameliorating both Aβ and Tau pathologies

Cong LI[1, 2], Xiao-dan GUO[2], Min LEI[2], Jia-yi WU[2], Jia-zhen JIN[2], Xiao-fan SHI[2], Zhi-yuan ZHU[2], Vatcharin RUKACHAISIRIKUL[3], Li-hong HU[2, *], Tie-qiao WEN[1], Xu SHEN[1, 2, *]

[1]*School of Life Sciences, Shanghai University, Shanghai 200444, China;* [2]*Key Laboratory of Receptor Research, Shanghai Institute of Materia Medica, Chinese Academy of Sciences, Shanghai 201203, China;* [3]*Department of Chemistry, Faculty of Science, Prince of Songkla University, Hat Yai, Songkhla 90112, Thailand*

Abstract

Considering the complicated pathogenesis of Alzheimer's disease (AD), multi-targets have become a focus in the discovery of drugs for treatment of this disease. In the current work, we established a multi-target strategy for discovering active reagents capable of suppressing both Aβ level and Tau hyperphosphorylation from natural products, and found that the ethanol extract of *Thamnolia vermicularis* (THA) was able to improve learning ability in APP/PS1 transgenic mice by inhibiting both Aβ levels and Tau hyperphosphorylation. SH-SY5Y and CHO-APP/BACE1 cells and primary astrocytes were used in cell-based assays. APP/PS1 transgenic mice [B6C3-Tg(APP_{swe}, PS1dE9)] were administered THA (300 $mg{\cdot}kg^{-1}{\cdot}d^{-1}$, ig) for 100 d. After the administration was completed, the learning ability of the mice was detected using a Morris water maze (MWM) assay; immunofluorescence staining, Congo red staining and Thioflavine S staining were used to detect the senile plaques in the brains of the mice. ELISA was used to evaluate Aβ and sAPPβ contents, and Western blotting and RT-PCR were used to investigate the relevant signaling pathway regulation in response to THA treatment. In SH-SY5Y cells, THA (1, 10, 20 μg/mL) significantly stimulated PI_3K/AKT/mTOR and AMPK/raptor/mTOR signaling-mediated autophagy in the promotion of Aβ clearance as both a PI_3K inhibitor and an AMPK indirect activator, and restrained Aβ production as a suppressor against PERK/eIF2α-mediated BACE1 expression. Additionally, THA functioned as a GSK3β inhibitor with an IC_{50} of 1.32±0.85 μg/mL, repressing Tau hyperphosphorylation. Similar effects on Aβ accumulation and Tau hyperphosphorylation were observed in APP/PS1 transgenic mice treated with THA. Furthermore, administration of THA effectively improved the learning ability of APP/PS1 transgenic mice, and markedly reduced the number of senile plaques in their hippocampus and cortex. The results highlight the potential of the natural product THA for the treatment of AD.

Keywords: Alzheimer's disease; *Thamnolia vermicularis*; SH-SY5Y cells; APP/PS1 transgenic mice; senile plaque; cognition; amyloid-β; Tau; autophagy; BACE1; GSK3β; PI_3K

Acta Pharmacologica Sinica (2017) 38: 9–28; doi: 10.1038/aps.2016.94; published online 3 Oct 2016

Introduction

Alzheimer's disease (AD) is a progressive neurodegenerative disease that is characterized by memory loss, cognitive decline and behavior disturbance and eventually leads to death[1]. AD is characterized by a complicated pathogenesis, and the accumulation of amyloid plaques that are composed of insoluble amyloid-β (Aβ) peptides and the formation of neurofibrillary tangles (NFTs) composed of hyperphosphorylated Tau proteins are two typical hallmarks of this disease[2]. Accordingly, targeting Aβ or Tau phosphorylation has been long believed to be a viable strategy for drug discovery against AD.

Aβ is generated from the sequential cleavage of amyloid-β precursor protein (APP) by β-site APP cleavage enzyme 1 (BACE1) and γ-secretase[3]. In the discovery of inhibitors of Aβ production, BACE1, as a rate-limiting enzyme for Aβ generation, has received much attention. However, no BACE1 inhibitor has passed clinical trials[4]. Recently, the down-regulation of BACE1 expression was suggested as a new approach for anti-AD drug discovery[5, 6] based on the fact that suppression of BACE1 expression efficiently improves AD symptoms[7, 8]. Apart from Aβ inhibiting production, promoting Aβ clearance

*To whom correspondence should be addressed.
E-mail xshen@simm.ac.cn (Xu SHEN);
lhhu@simm.ac.cn (Li-hong HU)
Received 2016-03-09 Accepted 2016-07-24

is also regarded as a valuable strategy in anti-AD research[9]. In this case, the discovery of autophagy activators has received major attention because autophagy is implicated to have an important role in Aβ clearance[10]. It has been discovered that activation of the mammalian target of rapamycin (mTOR) disrupts autophagy via phosphorylation of Unc51-like kinase 1 (ULK1), which is an initiator of the autophagy process[11], whereas AKT (protein kinase B, PKB) as a positive regulator of mTOR is regulated by phosphoinositide 3-kinase (PI_3-kinase, PI_3K)[12]. Therefore, the PI_3K/AKT/mTOR pathway is highly associated with autophagy-mediated Aβ clearance. Meanwhile, Tau hyperphosphorylation is believed to be the compelling cause of tauopathy and is regulated by a series of kinases and phosphatases[13], among which glycogen synthase kinase 3β (GSK3β) and cyclin-dependent kinase (CDK5) have been identified as the main kinases for Tau pathogenesis[14, 15].

Recently, in light of the failures in clinical trials for single-target anti-AD agents because of the complicated pathogenesis of this disease[16, 17], a multi-target-based strategy has been gradually accepted as a promising trend for the discovery of drug compounds against AD[18]. Therefore, it is expected that agents that are capable of inhibiting both Aβ levels and Tau hyperphosphorylation should be more potent anti-AD agents[19]. Accordingly, considering that natural products are major sources of bioactive agents based on their large-scale structural and acting target diversities, we have recently constructed a "one stone, two birds" platform against our laboratory's in-house natural product library to identify agents that are able to inhibit both Aβ levels and Tau hyperphosphorylation. As a result, THA, an extract of *Thamnolia vermicularis*, was discovered to improve learning ability in APP/PS1 transgenic mice by ameliorating Aβ/Tau pathology.

Thamnolia vermicularis mainly grows in snowy areas at altitudes 4000 m above sea level (*eg,* Yunnan and Sichuan Provinces of China) and is named "White snow tea" ("Baixuecha" in Chinese) in China[20]. *Thamnolia vermicularis* has been used in traditional Chinese medicine for many years[21], and pharmacological research has suggested that it has antioxidant and anticancer functions and can be used for the treatment of hypertension, cough, and neurasthenia[20, 22]. Recently, several phenolic compounds (*eg*, vermicularin, squamatic acid, barbatinic acid, *D*-arabitol, mannitol and baeomycesic acid) have been reported to be extracted from this type of lichen plant[23].

In the current work, we report that the ethanol extract of *Thamnolia vermicularis* (THA) improved learning ability in APP/PS1 transgenic mice by inhibiting both Aβ levels and Tau hyperphosphorylation. The mechanisms underlying the THA-mediated pharmacological events against AD were intensively investigated. Our results highlight the potential of THA in the treatment of AD.

Materials and methods

Materials

All cell culture reagents were purchased from Invitrogen. Complete protease inhibitor cocktail, Tween 80, Congo red, Thioflavine S and DMSO were from Sigma-Aldrich (MO, USA), and anti-Tau (phosphor S396) antibody was purchased from Abcam (MA, USA). Alexa Fluor488 goat anti-rabbit IgG (H+L) was purchased from Molecular Probes (Eugene, OR, USA). The antibodies against phospho-AKT(Ser473), AKT, phospho-PI_3K(p85/p55), PI_3K, phospho-AMPK (Thr172), AMPK, phospho-Raptor(Ser792), Raptor, phospho-mTOR (Ser2448), mTOR, phospho-P70S6K(Thr389), P70S6K, phospho-ULK(Ser757), ULK1, LC3II, p62, phospho-eIF2α (Ser51), eIF2α, phospho-GSK3β (Tyr216, Ser9), GSK3β, CDK5, p35/p25, Tau and GAPDH were purchased from Cell Signaling Technology (USA). The antibody against BACE1 was from Sigma-Aldrich (MO, USA), and the antibody against Aβ (6E10) was purchased from Biolegend (Covance).

Preparation of THA

THA was prepared according to a previously published method[24]. Briefly, *Thamnolia vermicularis* was collected in Yunnan Province of China in June 2009 and authenticated at Shanghai Institute of Materia Medica (SIMM), Chinese Academy of Sciences (Shanghai, China). A voucher sample (No TCM20080605) was deposited at Shanghai Research Center for Modernization of Traditional Chinese Medicine, SIMM.

Thamnolia vermicularis (2.0 kg) was extracted with 95% EtOH under reflux (20 L ×3) for 2 h. The extract was filtered, and the filtration was concentrated under reduced pressure to obtain 2 L of mixed suspension. The suspension was sedimentated for 5 h, followed by centrifugation at 4000 rounds per minute to yield a residue, and then dried to yield 150 g of the total phenolic acids. According to HPLC-UV analysis, the contents of squamatic acid (**1**) and baeomycesic acid (**2**) (Figure 1A) in the total phenolic acids were 42% and 46%, respectively.

Cell culture

In our current work, spontaneous over-expression of Aβ is needed for evaluating the Aβ inhibitory activity of the compound; therefore, the high Aβ expression of CHO-APP/BACE1 cells may facilitate the assay. According to the published reports, BV_2 microglia, a main immunocompetent cell in the CNS, functions potently in phagocytosing exogenous Aβ[25–27]. SH-SY5Y cells, a neuroblastoma cell line that closely resembles primary neurons, may be used instead of primary neurons[28–30], while primary astrocytes play an important role in autophagy-mediated Aβ clearance *in vivo* and are considered more suitable for the related assays[31–33]. Additionally, published reports have revealed that SH-SY5Y cells, as human neuroblastoma cells, are being widely used in the study of Tau pathology[28, 34, 35], and tauopathy was also discovered in glial cells and astrocytes[36, 37]. Thus, we used SH-SY5Y, BV_2 and astrocyte cells to study the regulation of THA against the signaling pathways involved in Aβ/Tau pathology. In addition, we did not use primary neurons because of their relatively low expression level of Aβ and the restricted number of cells[29, 32, 33]. As stated above, primary astrocytes play an important role in autophagy-mediated Aβ clearance *in vivo* and are considered more suitable for the related assay. Primary astrocytes were thus applied to further confirm the results obtained in the SH-

SY5Y cells.

SH-SY5Y cells were cultured in Dulbecco's modified Eagle's medium and Ham's F-12 (DMEM/F12) supplemented with 10% fetal bovine serum (FBS) and 100 unit/mL penicillin-streptomycin, and BV_2 cells were cultured in DMEM supplemented with 10% FBS and 100 unit/mL penicillin-streptomycin. CHO cells expressing APP and BACE1 (CHO-APP/BACE1) were cultured in F12 supplemented with 10% FBS and 100 unit/mL penicillin-streptomycin. Primary astrocytes were cultured in DMEM/F12 supplemented with 10% FBS and 100 unit/mL penicillin-streptomycin. All cells were cultured in a humidified incubator in 5% CO_2 at 37 °C.

ELISA assay

Aβ/sAPPβ content assay

CHO-APP/BACE1 cells were incubated with different concentrations of THA (20, 10, 1, or 0 mg/L) for 24 h, and the supernatant was collected, to which a complete protease inhibitor mixture was added (Thermo, USA). The contents of Aβ and sAPPβ were measured using human $Aβ_{40}$ (Invitrogen, KHB3481, USA) and sAPPβ (Immuno-Biological Laboratories, Japan) ELISA kits, respectively.

Aβ clearance assay

An exogenous Aβ clearance assay of the cells was performed according to the published Landreth approach[38, 39]. BV_2 cells, astrocytes and SH-SY5Y cells were incubated with different concentrations of THA (20, 10, 1, or 0 μg/mL) for 20 h and then treated with 2 μg/mL exogenous $Aβ_{40}$ or $Aβ_{42}$ for 3 h. Extracellular membrane exogenous Aβ was washed away three times using PBS buffer (pH 7.4), and the cells were then lysed in 50 mmol/L Tris buffer (pH 8.0) containing 5 mol/L guanidine hydrochloride. After the lysate was centrifuged at 20000×*g* for 30 min at 4 °C, the $Aβ_{40}$ and $Aβ_{42}$ in the supernatant were detected using human $Aβ_{40}$ and $Aβ_{42}$ ELISA kits, respectively.

Brains were assayed according to a previously published method[40]. Hippocampal and cortical samples were homogenized in 50 mmol/L Tris buffer (pH 8.0) containing 5 mol/L guanidine hydrochloride by manual grinding, followed by lysis at 4 °C for 1 h. The homogenates were centrifuged at 20000×*g* at 4 °C for 30 min, and the content of $Aβ_{40}$ or $Aβ_{42}$ in the supernatant was detected using human $Aβ_{40}$ or $Aβ_{42}$ ELISA kits, respectively.

In the assays, the total protein concentration of the sample was determined using a BCA protein assay kit (Thermo, USA), and all Aβ concentration values were normalized to the total protein concentration.

Western blotting

Cell-based assay

SH-SY5Y cells, BV_2 cells, CHO-APP/BACE1 cells and astrocytes were treated with varying concentrations of THA for 24 h and lysed with RIPA buffer (Thermo, USA) containing a protease inhibitor cocktail (Thermo, USA). Protein concentration was determined using a BCA protein assay kit (Thermo, USA). The lysis solutions were mixed with 2× loading buffer (4% SDS, 62.5 mmol/L Tris-HCI, pH 6.8, 25% glycerol, and 0.1% bromophenol blue), boiled for 15 min at 99 °C, and then centrifuged at 20000×*g* for 10 min.

Tissue-based assay

The cortices from four mouse brains in each group were homogenized by manual grinding in RIPA buffer (Thermo, USA) and kept on ice for 1 h to lyse completely. The homogenates were then centrifuged at 20000×*g* at 4 °C for 30 min. The total protein concentration of the supernatant was determined using a BCA protein assay kit (Thermo, USA). Equal amounts of homogenates (2 mg/mL protein) were mixed with 2× SDS-PAGE sample buffers, and equal amounts of mixture (3 mg/mL protein) were then boiled for 15 min at 99 °C followed by centrifugation at 20000×*g* for 10 min.

All samples prepared in cells and tissues were subject to Western blot analyses against PI_3K, phospho-PI_3K, AMPK, phospho-AMPK, AKT, phospho-AKT, Raptor, phospho-Raptor, mTOR, phospho-mTOR, P70S6K, phospho-P70S6K, ULK1, phospho-ULK1, BACE1, eIF2α, phospho-eIF2α, PERK, phospho-PERK, p62, Tau, phospho-Tau, GSK3β, phospho-GSK3β, CDK5, p35/p25, anti-Aβ, and GAPDH. The blots were visualized using a Dura detection system (Thermo, USA).

BACE1 activity assay

A BACE1 (β-secretase) activity kit (Invitrogen, USA) was used to determine the inhibition of THA against BACE1 activity *in vitro*. Briefly, BACE1 substrate (250 nmol/L), BACE1 enzyme (0.35 U/mL) and varied concentrations of THA were mixed gently and then incubated for 1 h at 37 °C in cells dark. The fluorescence intensity was measured at excitation and emission wavelengths of 545 and 585 nm, respectively.

PI_3K activity assay

Inhibition of THA on PI_3K enzymatic activity *in vitro* was assayed using a PI-3 kinase alpha (p110α/p85α) active assay kit (Echelon Biosciences Inc, USA) according to the manufacturer's protocol. In brief, PIP_2 substrate (10 μmol/L), PI_3K kinase (0.36 μmol/L) and various concentrations of THA were mixed and incubated for 3 h at room temperature, followed by the addition of 90 μL of kinase stop solution to stop the reaction. Then, 60 μL of cells reaction supernatant was transferred to a clean tube, followed by the addition of PIP_3 detector, and incubated for 1 h at room temperature. The absorbance at 450 nm was read. The result indicated that the colorimetric signal was inversely proportional to the amount of PI(3,4,5)P_3 produced by PI-3 kinase.

CDK5/P25 kinase enzyme assay

The effect of THA on CDK5/P25 kinase activity was determined using a CDK5/P25 Activity Assay Kit (Promega catalog #V3231) according to the manufacturer's protocol. Briefly, a CDK5 enzyme reaction system was directly incubated with different concentrations of THA or PHA-793887 (published

CDK5 inhibitor[41]) for 10 min, and then an ADP-GloTM Kinase Assay Kit (Promega catalog #V9101) was used to measure the activity of CDK5/P25 by quantifying the amount of ADP produced during the kinase reaction.

AMPK activity assay

The effect of THA on AMPK activity was determined using an ADP Hunter Plus Assay Kit (DiscoveRX, lot #13C1816), in which AMPK activity was investigated by quantifying the amount of ADP produced during the kinase reaction. In brief, varied concentrations of THA were incubated with AMPKα2β1γ1 (500 ng/mL) for 30 min on ice, followed by the addition of ATP (100 μmol/L) and SAMS (100 μmol/L) to start the reaction in cells dark. After 30 min, an ADP Hunter Plus Assay Kit was used to test ADP content. The fluorescence intensity was measured with excitation and emission wavelengths of 530 nm and 590 nm, respectively.

Autophagy activation by mRFP-GFP adenoviral vector

The effects of THA on autophagic flux and autolysosome formation were determined by using a confocal laser scanning microscope (CLSM)-based assay (HanBio, China), according to the provided kit protocol. Briefly, SH-SY5Y cells with an expression vector encoding mRFP-GFP fluorescence-tagged LC3 (mRFP-GFP-LC3) were incubated with different concentrations of THA or rapamycin (known autophagy inhibitor[42]) for 24 h at 37 °C. After cell fixation, the cells were imaged for green fluorescent protein (GFP) and red fluorescent protein (RFP) using an Olympus Fluoview FV1000 confocal microscope (Olympus, Japan). Autophagic flux was determined by evaluating the number of mRFP puncta (puncta/cell were counted).

Real-time PCR analysis

The total mRNA from cells and mouse brains was extracted using TRIzol Reagent according to the protocols of commercial kits. Complementary DNA synthesis was performed with oligo-dT primers according to the instructions of a reverse-PCR kit (TaKaRa Bio, Japan), and real-time PCR was carried out using SYBR Premix Ex Taq™ on a DNA Engine Opticon TM2 system (TaKaRa Bio, Japan). The primers used are listed in Table 1.

Animal experiments

All animal experiments were carried out according to the Institutional Ethical Guidelines of Shanghai Institute of Materia Medica, Chinese Academy of Sciences, on animal care. The APP/PS1 transgenic mice [B6C3-Tg (APP_{swe}, $PS1^{dE9}$)] were purchased from Jackson Laboratory (Bar Harbor, ME, USA) and fed in standard conditions of 12 h of light/day at a room temperature of 22 °C. Twenty male APP/PS1 transgenic mice were randomly divided into two groups, and ten non-transgenic mice were used as a negative control group. THA was dissolved in 0.9% sodium chloride injection containing 5% Tween 80. The two 6-month APP/PS1 transgenic groups were given 300 mg THA/kg per day or vehicle by intragastric administration, and the 6-month non-transgenic group was given vehicle through intragastric administration. After 100 d of administration, the learning ability of the mice was detected using Morris water maze (MWM) assay. Upon completion of the MWM test, all mice were immediately euthanized, and all brains were removed and bisected in the mid-sagittal plane. The left sides of the brains were fixed in 4% paraformaldehyde for histologic analysis, and the right sides of the brains were stored at -80 °C.

Table 1. Primer sequences.

Gene	Sequences
Human BACE1	forward primer 5′-AGGGCTTGCACCTGTAGGAC-3′
	reverse primer 5′-GCCTGAGTATGACGCCAGTA-3′
Mice BACE1	forward primer 5′-CCGGCGGGAGTGGTATTATGAAGT-3′
	reverse primer 5′-GATGGTGATGCGGAAGGACTGATT-3′
Human β-actin	forward primer 5′-CTCCATCCTGGCCTCGCTGT-3′
	reverse primer 5′-GCTGTCACCTCCACCGTTCC-3′
Mice GAPDH	forward primer 5′-ACAGCAACAGGGTGGTGGAC-3′
	reverse primer 5′-TTTGAGGGTGCAGCGAACTT-3′

MWM assay

MWM assay was used to determine the cognitive ability of mice, as described in a previously published report[40]. Briefly, each mouse was given 90 s for 3 trials per day for 9 consecutive days to find the invisible submerged white platform in a circular pool (120 cm in diameter, 50 cm deep) filled with milk-tinted water using a variety of visual cues located on the pool wall. The mice were allowed to stay on the platform for 15 s if the mice found the platform within 90 s. However, if the mice failed to find the platform within 90 s, the mice were guided to find the platform and were allowed to stay on the platform for 15 s. All data were collected for the mouse performance analysis. The escape latency, which is the amount of time the mouse takes to find the platform, is a major parameter for cognitive evaluation and thus was calculated every day.

Congo red and Thioflavine S staining

The paraformaldehyde-fixed brain tissues (~3.5 mm thick) containing the hippocampus and cortex were embedded in paraffin. Ten-micrometer-thick coronal sections were used for Congo red and Thioflavine S staining, according to a previously described approach[40].

Nine sections (10 mm thick) were produced per mouse, and each group comprised 4 mice. For Congo red staining, the sections were deparaffinized, hydrated and stained in Congo red for 20 min, and then differentiated in alkaline alcohol solution, followed by counterstaining with Gill's hematoxylin for 30 s, and finally mounting with neutral gum. The total number of Congo red stained plaques in the hippocampus and cortex (4 mice per group) was separately calculated for the statistical

analysis.

For Thioflavine S staining, the sections were deparaffinized, hydrated and stained in 1% Thioflavine S for 5 min, then differentiated in 70% alcohol solution for 5 min, followed by mounting with glycerol gel. The number of Thioflavine S plaques was counted for every three to six fields throughout the entire hippocampus and cortex (4 mice per group) using Image-Pro Plus (Media Cybernetics).

Immunofluorescence staining

The sections described as before[40], embedded in paraffin, were prepared for immunofluorescence staining. Nine sections (10 mm thick) were produced per mouse, and each group comprised 4 mice. After being deparaffinized and hydrated, the sections were incubated in PBS for 2 min, followed by incubation with 3% hydrogen peroxide (H_2O_2). Then, citric acid (pH 6.0) was used for antigen retrieval of the sections submitted to microwave heating at medium heat for 6 min, followed by natural cooling to room temperature, for 4 times. Then, the sections were blocked with PBS-0.05% Triton-X 100-10% horse serum for 10–30 min and incubated with primary antibody overnight at 4 °C in PBS-0.05% Triton X-100-1% horse serum, and then the sections were incubated in primary antibody at RT for 45 min. The sections were subsequently rinsed with PBS 3 times (3 min/time) and incubated for 45 min in secondary rabbit antibody Alexa Flour® 488 goat anti-rabbit IgG (H+L) (PBS-0.05%Triton X-100-1% horse serum). The images were acquired using a laser scanning confocal microscope (Nikon, Japan).

Wild-type *Drosophila melanogaster* culture and lifespan assays

yw D *melanogaster* isogenic Canton-S flies (outcrossed with wlll8 (isoCJ1) for 5 generations) were used in the experiments by JoeKai company. All flies were bred on standard cornmeal food and were originally reared at 23–25 °C and 40%–60% relative humidity (RH) on a 12 h–12 h light-dark cycle. On the second day after eclosion (DAE), male flies were selected and stored separately into different vials (15 flies/vial) for the drug feeding process (25 °C, 40%±15%). Initially, there were at least 225 flies for each condition. One day before drug feeding, approximately 1 mg compound was diluted to 0.05 or 0.005 mg/mL with 4% sucrose and 5% Tween-80 working solutions. At DAE3, the flies were treated with drugs for 4 h after 2 h of starvation, followed by 18 h of rest in a fresh food vial. On each feeding day, 40 μL drug or vehicle solutions were delivered to each vial. Dead flies were recorded on a daily basis until all flies had died. All statistical analysis was performed using SPSS version 20 (IBM).

Statistical analysis

Significant differences between multiple treatments and controls were analyzed using one-way ANOVA followed by Bonferroni's *post hoc* test. Differences between double variants were analyzed with two-way ANOVA followed by Bonferroni's *post hoc* test. *P* values of less than 0.05 were considered to be significant.

Results

THA inhibits both Aβ level and Tau hyperphosphorylation

Compound screening

To screen for the natural product extracts that exhibit multifunctional activities in inhibiting both Aβ levels and Tau hyperphosphorylation, an ELISA assay[43] was first applied to screen for extracts active in inhibiting Aβ levels. The ELISA assay was performed using our laboratory's in-house natural product extract library (~230 extracts) in CHO-APP/BACE1 cells, and THA was finally discovered. THA was then determined to exhibit ability to inhibit Tau hyperphosphorylation in both SH-SY5Y and primary neuronal cells.

THA decreased Aβ levels

To evaluate the inhibition of THA against Aβ levels, CHO-APP/BACE1 cells were incubated with different concentrations of THA (20, 10, 1, or 0 μg/mL), and $Aβ_{40}$ levels in the cell culture medium were detected by ELISA assay. As shown in Figure 1B, THA treatment markedly decreased Aβ levels in the cells.

THA reduced Tau phosphorylation

Inhibition of THA against Tau hyperphosphorylation (Ser 396) was inspected by Western blot assays in SH-SY5Y cells (Figure 1C, 1F), BV_2 cells (Figure 1D, 1F) and primary astrocytes (Figure 1E, 1F). The results showed that THA reduced Tau hyperphosphorylation in the cells.

THA inhibits Aβ production involving alleviation of PERK/eIF2α signaling-mediated BACE1 expression

THA inhibited Aβ production

Given that the Aβ level involves a balance of Aβ production and clearance[44], we investigated whether the THA-induced Aβ inhibition was achieved through inhibition of Aβ production and/or promotion of Aβ clearance. We first examined the level of sAPPβ, a direct product of APP upon β-cleavage[44], in CHO-APP/BACE1 cells by ELISA assays. As indicated in Figure 2A, THA effectively reduced sAPPβ in the CHO-APP/BACE1 cells, indicative of its inhibition of Aβ production.

THA inhibited Aβ production involving alleviation of PERK/eIF2α signaling-mediated BACE1 expression

Next, we sought to explore the mechanism underlying the THA-induced suppression of Aβ production. Given that BACE1 is the key rate-limiting enzyme responsible for Aβ production[4], we focused on the regulation of THA against BACE1 relating to its enzymatic activity and protein expression. Interestingly, THA had no effects on BACE1 enzymatic activity *in vitro* (Figure 2B, TDC as a positive control[40]) but decreased sAPPβ and BACE1 protein levels in CHO-APP/BACE1 cells (Figure 2C, 2F) and primary astrocytes (Figure 2D, 2G), as indicated by Western blot results. Accordingly, we investigated the THA-mediated regulation of BACE1 transcription and/or translation in response to its inhibition against BACE1 expression. Considering that THA had no effects on BACE1 transcription, according to the RT-

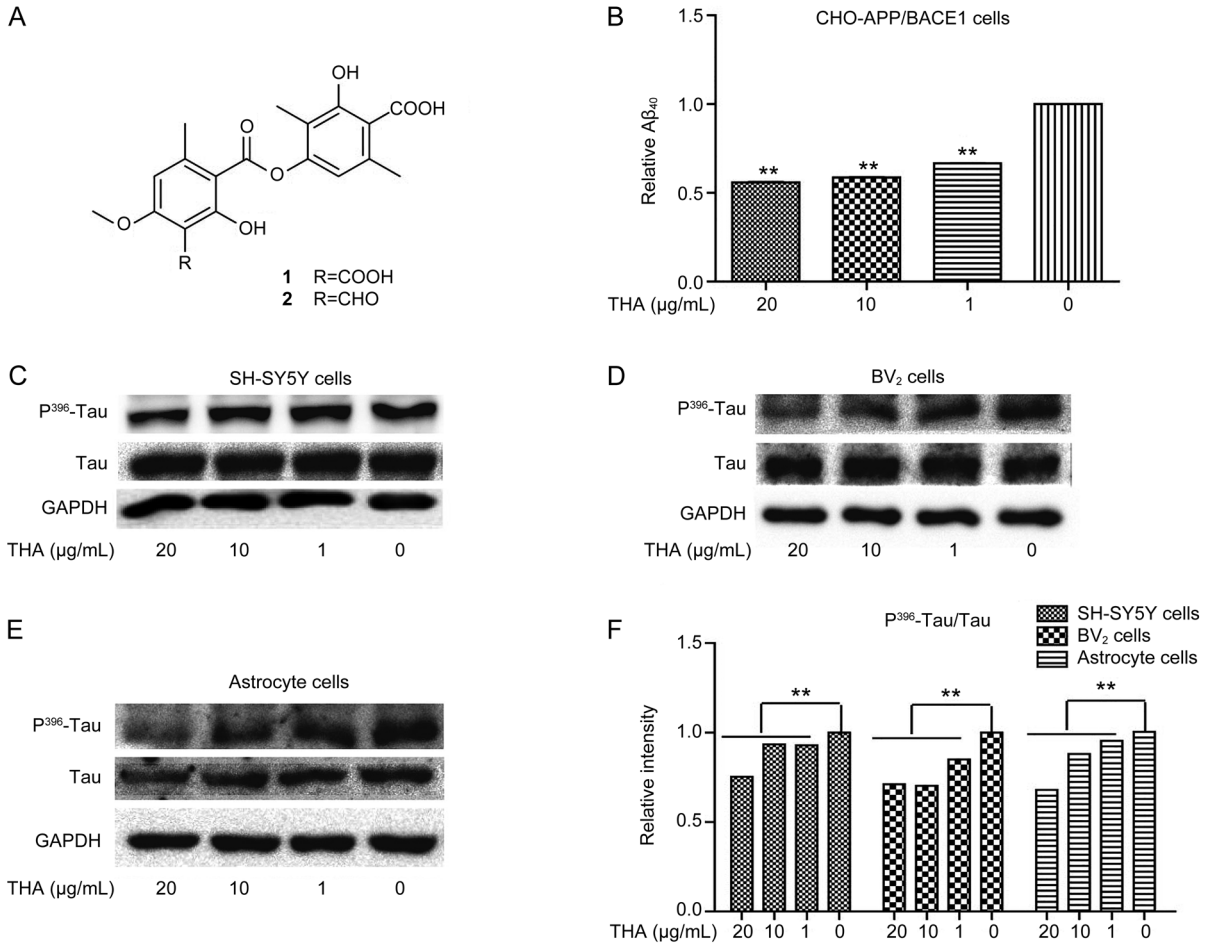

Figure 1. THA inhibited Aβ deposition and Tau hyperphosphorylation. (A) In THA, the contents of squamatic acid (**1**) and baeomycesic acid (**2**) are 42% and 46%, respectively. (B) CHO-APP/BACE1 cells were cultured with different concentrations of THA (20, 10, 1, or 0 μg/mL) for 24 h, and $Aβ_{40}$/sAPPβ levels were detected via ELISA assays of the supernatants. (C–E) Cells were cultured with different concentrations of THA (20, 10, 1, or 0 μg/mL) for 24 h, and P^{396}-Tau was detected by Western blot assays in SH-SY5Y cells (C), BV_2 cells (D), and astrocytes (E). (F) Densitometry analysis of Figures C–E. GAPDH was used as a loading control in the Western blot assays. The results were obtained from three independent experiments. Values are the mean±SEM, one-way ANOVA, Bonferroni's multiple comparison test. n=3. $^{**}P$<0.01 compared with the control group, control group: 0 μg/mL THA treatment group.

PCR assay (Figure 2E), we focused on the regulation of THA against BACE1 translation. In light of the fact that PERK/eIF2α signaling is highly implicated in BACE1 translation[45], we inspected whether THA regulated PERK/eIF2α signaling. As expected, the Western blot results demonstrated that THA diminished the phosphorylation of PERK and eIF2α in CHO-APP/BACE1 cells (Figure 2C, 2F) and astrocytes (Figure 2D, 2G).

Thus, our results indicated that THA inhibited Aβ production and this process involved the alleviation of PERK/eIF2α signaling-mediated BACE1 expression.

THA promotes Aβ clearance involving activation of both PI_3K/AKT/mTOR and AMPK/Raptor/mTOR signaling-mediated autophagy

THA promoted Aβ clearance

Next, we investigated the potential of THA in the promotion of Aβ clearance. The assay was carried out in SH-SY5Y cells (Figure 3A, 3B), BV_2 cells (Figure 3C, 3D) and primary astrocytes (Figure 3E, 3F). As indicated, THA markedly enhanced exogenous $Aβ_{42}/Aβ_{40}$ clearance in the cells, indicative of the promotion of THA on Aβ clearance. According to a published report, Cu^{2+} binds to Aβ[46, 47] and promotes fiber formation[48]. Here, to exclude the possibility that the inhibition of exogenous Aβ by THA treatment was a result of a direct reaction between Aβ and THA, we performed the related ELISA assays by using Cu^{2+} as a positive control *in vitro*. As demonstrated in Supplementary Figure S1A, incubation of THA did not reduce exogenous Aβ, and Cu^{2+} treatment markedly reduced Aβ levels. This result thereby implied that the THA-induced inhibition of exogenous Aβ was not due to a direct extracellular reaction between Aβ and THA.

In addition, to prove that THA did not impair the cellular function of Aβ endocytosis resulting in the decline of "intracel-

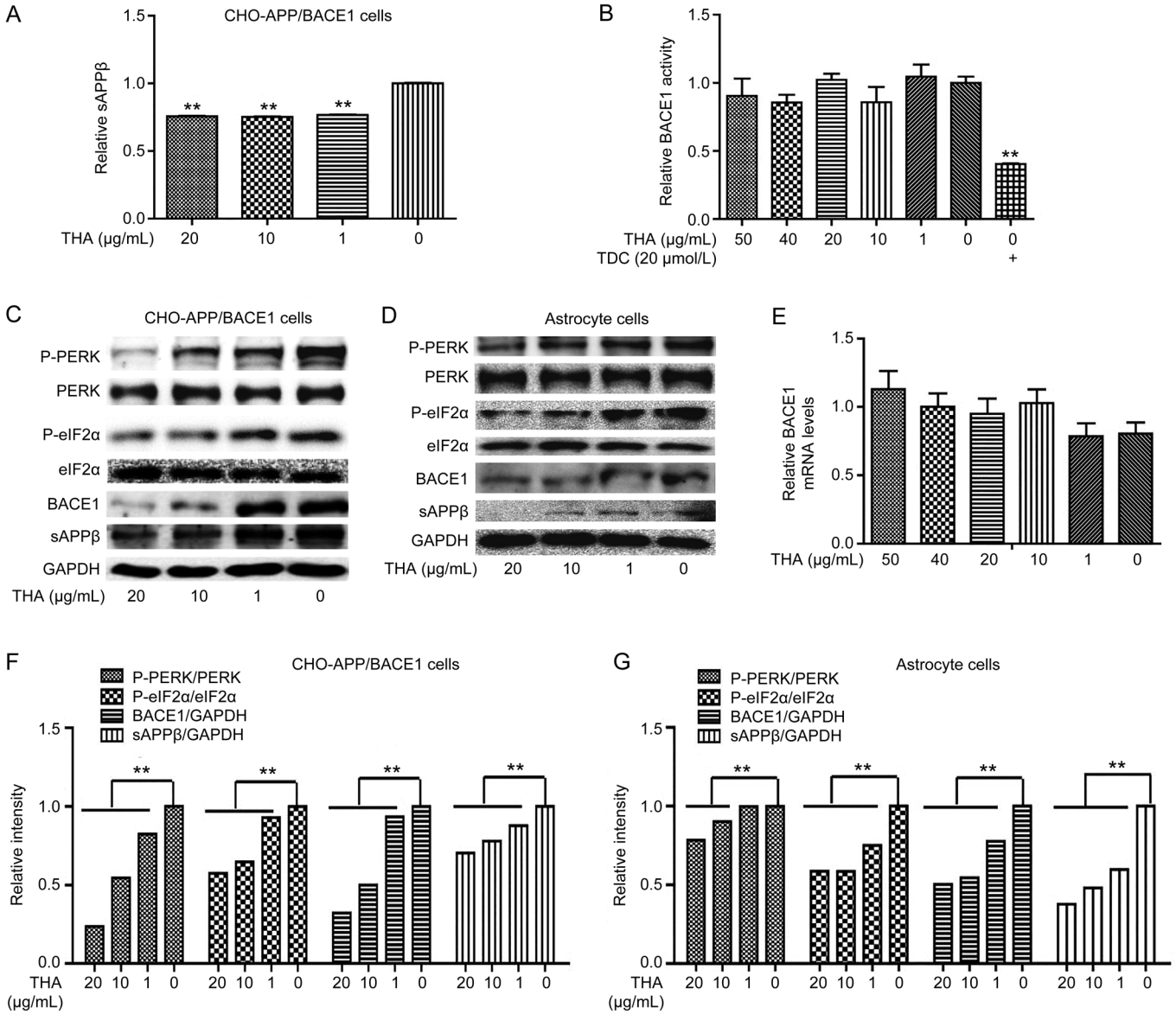

Figure 2. THA decreased Aβ production by inhibiting BACE1 translation in CHO-APP/BACE1 cells and astrocytes. (A) CHO-APP/BACE1 cells were cultured with different concentrations of THA (20, 10, 1, or 0 μg/mL) for 24 h, and sAPPβ levels were detected by ELISA assays in the supernatant. (B) A FRET-based BACE1 enzyme reaction system was directly incubated with different concentrations of THA (20, 10, 1, or 0 μg/mL), and an *in vitro* BACE1 activity was then evaluated. (TDC: 2,2′,4′-trihydroxychalcone, BACE1 non-competitive inhibitor[45]). (C, D) Cells were cultured with different concentrations of THA (20, 10, 1, 0 or μg/mL) for 24 h, and levels of eIF2α and PERK was detected by Western blot assays in the CHO-APP/BACE1 cells (C) and astrocytes (D). (E) An RT-PCR assay was used to test the effect of THA on BACE1 transcription. (F) Densitometry analysis of Figure (C). (G) Densitometry analysis of Figure (D). GAPDH was used as a loading control in the Western blot assays. The results were obtained from three independent experiments. Values are the mean±SEM, one-way ANOVA, Bonferroni's multiple comparison test. n=3. $^{**}P$<0.01 compared with the control group, control group: 0 μg/mL THA treatment group.

lular" Aβ, we also performed the relevant assays in SH-SY5Y cells, in which we examined Aβ levels in the supernatant and cell lysis by ELISA (Supplementary Figure S1B, S1C, Figure 3A, 3B). The results indicated that THA reduced Aβ levels both in the supernatant (Supplementary Figure S1B, S1C) and the cell lysis (Figure 3A, 3B), which thus indirectly demonstrated that THA rendered no impairment on the cellular function of Aβ endocytosis.

THA activated autophagy

Given that autophagy, a major degradation process for abnormal and aggregated proteins, plays an important role in Aβ clearance[49], we next investigated the potential of THA in the regulation of autophagy.

First, an mRFP-GFP adenoviral infection-based assay[50, 51] was carried out to examine the effect of THA on autophagy flux and autolysosome formation in SH-SY5Y cells with an

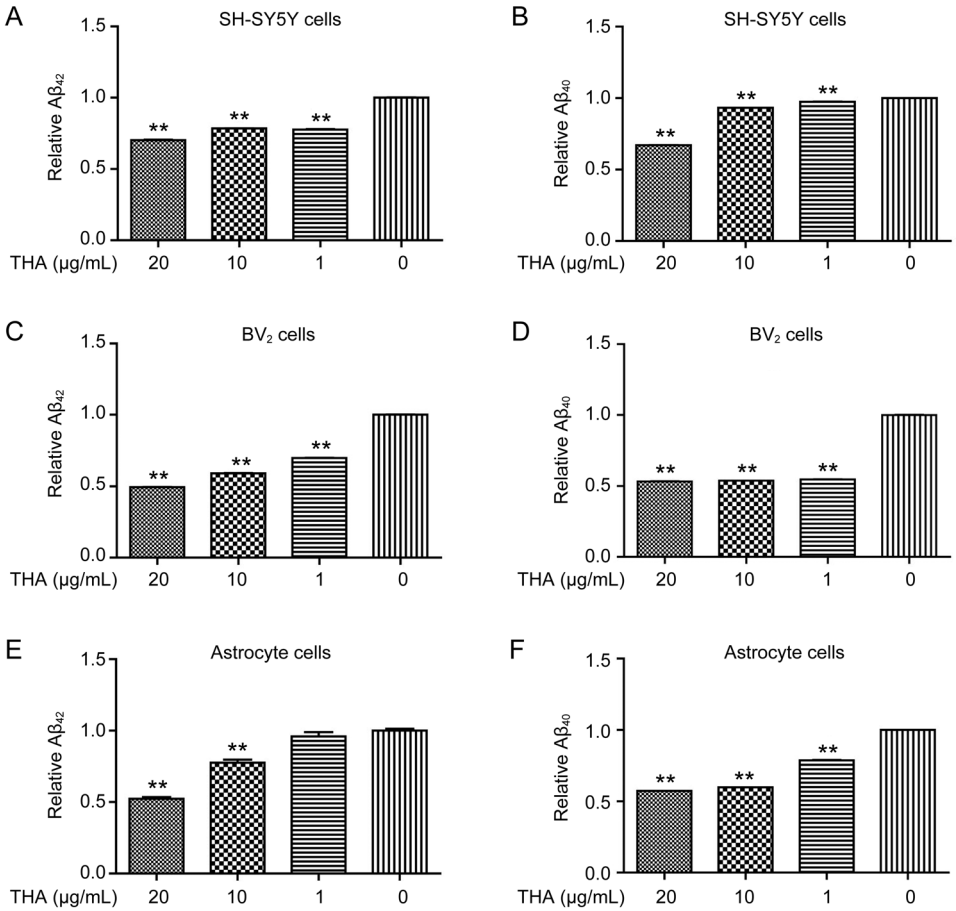

Figure 3. THA promoted Aβ clearance. (A–F) Cells were cultured with different concentrations of THA (20, 10, 1, or 0 μg/mL) for 20 h and treated with 2 μg/mL soluble $Aβ_{40/42}$ for 3 h. Intracellular $Aβ_{40/42}$ was evaluated by an ELISA assay and normalized to the total protein in SH-SY5Y cells (A, B), BV_2 cells (C, D) and astrocytes (E, F). The results shown correspond to three independent experiments. Values are the mean±SEM, one-way ANOVA, Bonferroni's multiple comparison test. n=3. $^{**}P$<0.01 compared with the control group, control group: 0 μg/mL THA treatment group.

expression vector encoding mRFP-GFP fluorescence-tagged LC3 (microtubule-associated protein light chain 3) (mRFP-GFP-LC3). As indicated in Figure 4A, 4B, THA increased the puncta of mRFP-Red-LC3 and mRFP-GFP-yellow-LC3, thus demonstrating that THA effectively promoted autophagy flux and autolysosome formation.

In addition, Western blot assay was also performed to further verify the activation of THA on autophagy in SH-SY5Y cells (Figure 4C, 4F), BV_2 cells (Figure 4D, 4G) and primary astrocytes (Figure 4E, 4H) by testing several key marker proteins of autophagy, including Unc51-like kinase 1 (ULK1), LC3II and polyubiquitin binding protein p62[52]. The results demonstrated that THA reduced phosphorylated ULK1 and increased LC3II protein levels in all three tested cells. It was noted that THA suppressed p62 levels in both SH-SY5Y cells and primary astrocytes, but had no effects on BV_2 cells, possibly due to the cellular selectivity of THA, similar to the case of a previously published report[43]. Thus, these results indicated that THA activated autophagy in the cells.

THA alleviates Aβ levels involving autophagy activation

Next, ELISA assay was carried out to verify the activity of THA in reducing Aβ levels via autophagy activation by incubating cells with the autophagy inhibitor chloroquine (CQ[53]). In the assay, CHO-APP/BACE1 cells were treated with THA (20 μg/mL), vehicle alone, CQ (10 μmol/L), or THA in combination with CQ for 24 h. The results in Figure 4I demonstrated that CQ effectively reversed the THA-induced decrease in Aβ levels. This result indicated that THA reduced Aβ levels involving autophagy activation.

THA-induced autophagy promotion involves both PI_3K/AKT/mTOR and AMPK/Raptor/mTOR signaling pathways

Because we determined the capability of THA in stimulating autophagy, we next explored its underlying mechanisms. Given the report that the PI_3K/AKT/mTOR and AMPK/Raptor/mTOR signaling pathways are tightly implicated in autophagy[54], we carried out the related assays to investigate the potential regulation of THA against these two pathways in response to the THA-induced autophagy stimulation in SH-

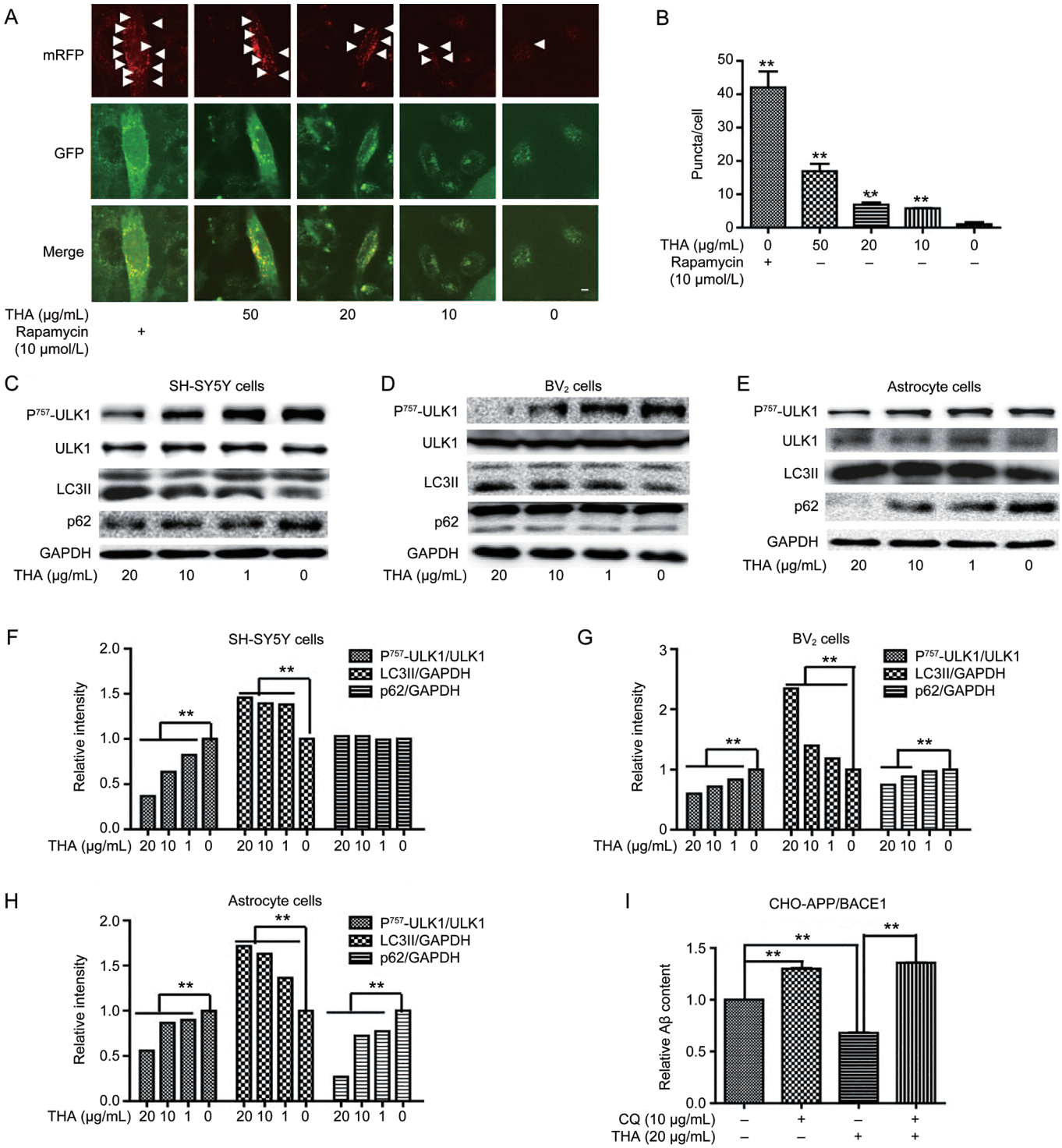

Figure 4. THA produced Aβ clearance by activating autophagy. (A) CLSM images of SH-SY5Y cells transiently expressing mRFP-GFP-LC3 (Red puncta indicate mRFP, pointed with white arrows). Scale bar: 5 μm. (B) Statistics of image (A) one-way ANOVA, Bonferroni's multiple comparison test. n=3. $^{**}P$<0.01. (C–H) Cells were cultured with different concentrations of THA (20, 10, 1, or 0 μg/mL) for 24 h, and marker proteins of autophagy, including Unc51-like kinase 1 (ULK1), LC3II and polyubiquitin binding protein p62, were detected by Western blot assays in SH-SY5Y cells (C), BV_2 cells (D) and primary astrocytes (E). (F) Densitometry analysis of Figure (C), one-way ANOVA, Bonferroni's multiple comparison test. n=3. $^{**}P$<0.01. (G) Densitometry analysis of Figure (D), one-way ANOVA, Bonferroni's multiple comparison test. n=3. $^{**}P$<0.01. (H) Densitometry analysis of Figure (E). GAPDH was used as a loading control in the Western blot assays, one-way ANOVA, Bonferroni's multiple comparison test. n=3. $^{**}P$<0.01. (I) CHO-APP/BACE1 cells were treated with THA (20 μg/mL), vehicle alone, CQ (10 μmol/L), or THA in combination with CQ for 24 h, and the Aβ levels in the cell culture media were tested by ELISA (t test. n=3. $^{**}P$<0.01 compared with the control group). The results were obtained from three independent experiments. Values are the mean±SEM. n=3. $^{**}P$<0.01 compared with the control group, control group: 0 μg/mL THA treatment group.

SY5Y cells (Figure 5A–5D), BV_2 cells (Figure 5E–5I) and primary astrocytes (Figure 5J–5M) by Western blot.

As expected, the results demonstrated that THA decreased the phosphorylation of mTOR, PI_3K and AKT, whereas it increased the phosphorylation of AMPK and Raptor in all three tested cells. THA suppressed P70S6K phosphorylation in both SH-SY5Y cells and primary astrocytes but had no effects on BV_2 cells, probably due to the cellular selectivity of THA. Thus, these results indicated that THA activated autophagy by regulating both the PI_3K/AKT/mTOR and AMPK/Raptor/mTOR signaling pathways.

THA functions as both a PI_3K inhibitor and an indirect AMPK activator

Because we determined that THA inhibited PI_3K phosphorylation and stimulated AMPK phosphorylation, we next investigated whether THA functioned as an inhibitor against the PI_3K enzyme and as an activator of the AMPK enzyme. *In vitro* enzymatic activity assays were carried out, which demonstrated that THA directly inhibited PI_3K enzyme activity but rendered no effects on AMPK enzyme (Figure 5N, 5O. Wortmannin: PI_3K inhibitor[55]; A769662: AMPK activator[56]). Therefore, THA functioned as both a PI_3K inhibitor and an indirect AMPK activator.

THA reduces Tau hyperphosphorylation by functioning as a GSK3β inhibitor

It was reported that glycogen synthase kinase 3β (GSK3β) and cyclin-dependent kinase 5 (CDK5) are the two main kinases for Tau pathogenesis[14, 15]. GSK3β is activated when its Tyr216 is phosphorylated or its Ser9 is de-phosphorylated, thus enhancing Tau phosphorylation[14]. CDK5 is activated by p35 or p25 (the cleaved product of p35) to stimulate Tau phosphorylation[15]. Given these facts, we next performed Western blot assays to investigate the regulation of THA against GSK3β and CDK5. The results indicated that THA effectively decreased GSK3β Tyr216 phosphorylation without affecting its Ser9 phosphorylation and failed to affect CDK5 or p35/p25 in SH-SY5Y cells (Figure 6A, 6D), BV_2 cells (Figure 6B, 6E) or primary astrocytes (Figure 6C, 6F).

Furthermore, *in vitro* CDK5 and GSK3β enzyme activity assays were also performed. The results demonstrated that HTA had no effects on CDK5 enzymatic activity (Figure 6G, PHA-793887: CDK5 inhibitor[41]) but inhibited GSK3β enzymatic activity with an IC_{50} of 1.32±0.85 μg/mL (Figure 6H). Therefore, all these results suggested that THA reduced Tau phosphorylation by functioning as a GSK3β inhibitor.

THA ameliorates space learning ability in APP/PS1 transgenic mice

It has been reported that APP/PS1 transgenic mice may express chimeric mouse/human Swedish mutant amyloid precursor protein and mutant human presenilin 1 protein and that they exhibit obvious age-related memory impairments and Aβ accumulation and deposition. These mice have been largely regarded as an appropriate model for AD-related research[57]. Given that THA was effective in both decreasing Aβ content and attenuating Tau pathology in cells, we next examined the potential of THA in the improvement of space learning ability in APP/PS1 transgenic mice by performing a MWM assay[58].

The results demonstrated that in the training trials, the escape latencies of the non-transgenic vehicle group to find the platform were significantly shorter compared with the transgenic AD model vehicle group (Figure 7A, 7B), indicating that the space learning ability of the transgenic AD model mice were obviously impaired. However, the latencies of the THA-administered (300 $mg\cdot kg^{-1}\cdot d^{-1}$) transgenic AD model group were significantly decreased compared with the transgenic vehicle group (Figure 7A, 7B). We chose two doses of THA, 100 and 300 $mg\cdot kg^{-1}\cdot d^{-1}$, for this study. Because THA at 100 $mg\cdot kg^{-1}\cdot d^{-1}$ exhibited no effect, we omitted this dosage in the text. These results suggested that THA ameliorated the space learning ability of APP/PS1 transgenic mice.

THA reduces senile plaque formation in APP/PS1 transgenic mice

Congo red and Thioflavine S staining assays

Aβ-formed senile plaques are one of the major hallmarks of AD, and the progressive deposition of these plaques in the hippocampus and cortex results in space learning memory impairment[59]. As our results demonstrated that THA ameliorated space learning impairments in APP/PS1 transgenic mice, we next inspected whether THA alleviated senile plaque formation in the hippocampus and cortex of the tested transgenic mice by Congo red (Figure 8A–8D) and Thioflavine S staining (Figure 8E–8H) assays.

After the MWM test, the mice were sacrificed, and the left sides of the brains were immediately fixed in 4% paraformaldehyde for histological analysis. As expected, the numbers of Congo red (Figure 8A–8D)-stained senile plaques in both the hippocampus and cortex of the vehicle-administered transgenic mice were greater than in the vehicle-administered non-transgenic mice. However, treatment with THA (300 $mg\cdot kg^{-1}\cdot d^{-1}$) could effectively reverse the high senile plaque numbers in both the hippocampus and cortex of the transgenic mice. Similarly, the Thioflavine S staining assay results (Figure 8E-8H) also confirmed the inhibition of THA against senile plaque formation in the transgenic mice. The senile plaque burdens stained by Thioflavine S in the hippocampus and cortex of the vehicle-administered transgenic mice were markedly more severe compared with those of vehicle-administered non-transgenic mice, whereas treatment with THA reversed the senile plaque formation in the transgenic mice.

ELISA assay

To further investigate the inhibitory activity of THA on Aβ-formed senile plaques, we also inspected the effect of THA on $Aβ_{40}$/$Aβ_{42}$ levels in hippocampal and cerebral cortical homogenates by an ELISA assay. As shown in Figure 8I–8L, $Aβ_{40}$/$Aβ_{42}$ levels in both the hippocampus and cerebral cortex of the transgenic mice were higher compared with those

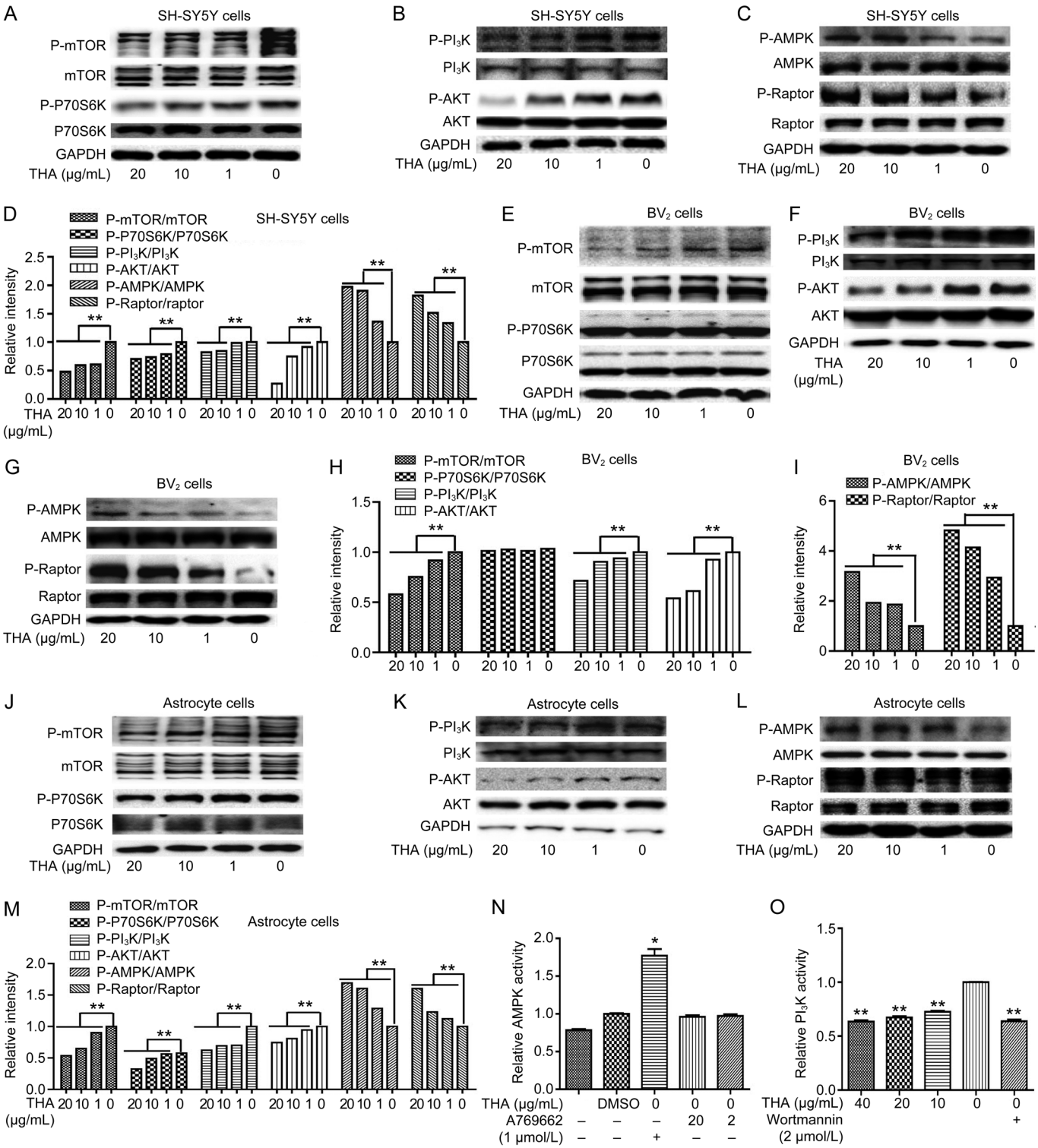

Figure 5. Inhibition of PI_3K/AKT and activation of the AMPK/Raptor pathway were involved in promotion of THA-mediated Aβ clearance. (A–M) Cells were cultured with different concentrations of THA (20, 10, 1, or 0 μg/mL) for 24 h, and the levels of P-mTOR, mTOR, P-P70S6K, P70S6K, P-PI_3K, PI_3K, P-AKT, AKT, P-AMPK, AMPK, P-Raptor, and Raptor were detected by Western blot in SH-SY5Y cells (A–C), BV_2 cells (E–G) and astrocytes (J–L). (D) Densitometry analysis of Figures (A–C). (H) Densitometry analysis of Figure (E and F). (I) Densitometry analysis of Figure (G). (M) Densitometry analysis of Figures (J–L). (N) An AMPK enzyme reaction system was directly incubated with different concentrations of THA (20 or 2 μg/mL), and the *in vitro* AMPK activity was then evaluated. A769662: AMPK activator[56]. (O) A PI_3K enzyme reaction system was directly incubated with different concentrations of THA (40, 20, 10, or 0 μg/mL), and the *in vitro* PI_3K activity was then evaluated. Wortmannin: PI_3K inhibitor[55]; GAPDH was used as a loading control in the Western blot assays. The results were obtained from three independent experiments. Values are the mean±SEM, one-way ANOVA, Bonferroni's multiple comparison test. n=3. $^{*}P$<0.05, $^{**}P$<0.01 compared with the control group, control group: 0 μg/mL THA treatment group.

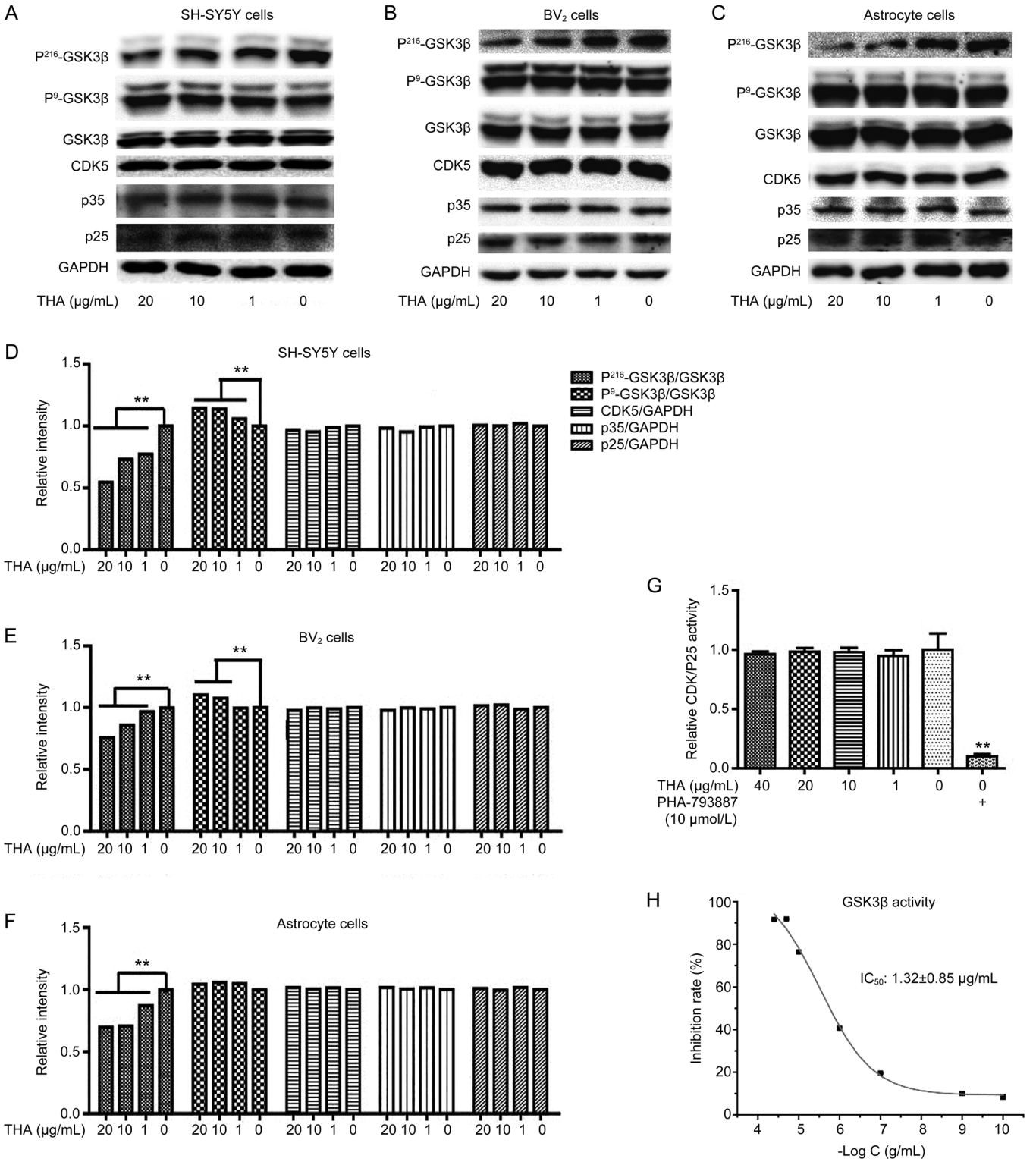

Figure 6. THA was a GSK3β inhibitor. (A–C) The levels of P^{216}-GSK3β, P^{9}-GSK3β, GSK3β, CDK5, and p35/p25 were detected by Western blot assays in SH-SY5Y cells (A), BV_2 cells (B) and primary astrocytes (C). (D) Densitometry analysis of Figure (A). (E) Densitometry analysis of Figure (B). (F) Densitometry analysis of Figure (C). (G) CDK5 enzyme reaction system was directly incubated with different concentrations of THA (50, 40, 20, 10, 1, or 0 mg/L) and *in vitro* CDK5 activity was then evaluated. PHA-793887: CDK5 inhibitor[41]. (H) GSK3β enzyme reaction system was directly incubated with different concentrations of THA (40, 20, 10, 1, 0.1, 0.001, or 0.0001 μg/mL), and the *in vitro* GSK3β activity was then evaluated. THA inhibited GSK3β enzymatic activity with an IC_{50} of 1.32±0.85 mg/L. GAPDH was used as a loading control in the Western blot assays. The results correspond to three independent experiments. Values are the mean±SEM, one-way ANOVA, Bonferroni's multiple comparison test. n=3. $^{**}P$<0.01 compared with the control group, control group: 0 mg/L THA treatment group.

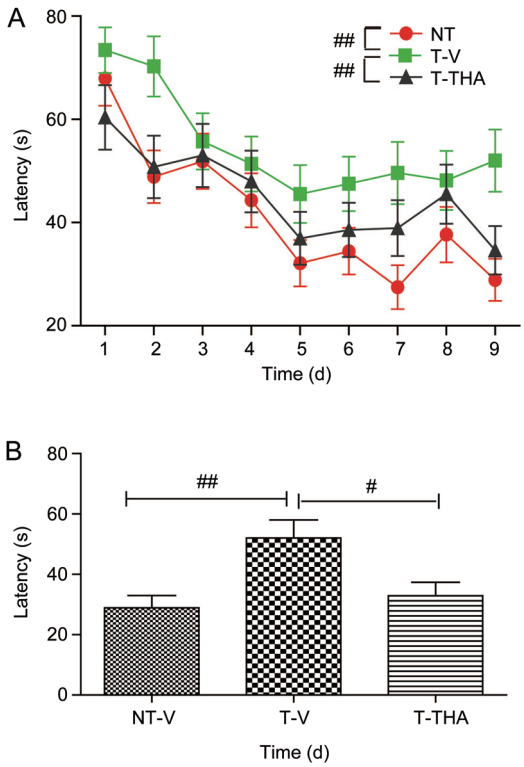

Figure 7. THA ameliorated space learning ability in the APP/PS1 transgenic mice. The MWM test was used to evaluate the effect of THA on the space learning ability of the AD model mice. (A) In training trials, the escape latencies to find the platform were measured to evaluate the memory ability of the mice (two-way ANOVA, Bonferroni's *post hoc* test. n=10. $^{\#\#}P$<0.01 compared with T-V). (B) Statistical analysis of (A) in for nine days of latency (t test. n=10. $^{\#}P$<0.05, $^{\#\#}P$<0.01 compared with T-V). NT-V, non-transgenic vehicle group; T-V, transgenic AD model vehicle group; T-THA, transgenic AD model with THA administration (300 mg·kg^{-1}·d^{-1}) group. Values are the mean±SEM.

of the non-transgenic mice, and administration of THA (300 mg·kg^{-1}·d^{-1}) efficiently decreased $A\beta_{40}/A\beta_{42}$ levels in both the hippocampus and cerebral cortex of the transgenic mice compared with those of the vehicle-treated transgenic group. In addition, we also performed Western blot assay[60, 61] to detect the effect of THA on Aβ polymer in the cells and the cortex (Supplementary Figure S1D–S1G), and the results indicated that THA had no effects on Aβ polymer. Thus, these results suggested that THA may downregulate soluble Aβ to reduce the levels of Aβ plaques in APP/PS1 transgenic mice.

THA alleviates PERK/eIF2α-mediated BACE1 translation in response to Aβ production inhibition in APP/PS1 transgenic mice

Given that THA repressed PERK/eIF2α-mediated BACE1 translation in response to Aβ production inhibition in cells, we next confirmed the effect in APP/PS1 transgenic mice.

In the assay, we detected the effects of THA on the protein level of sAPPβ/BACE1 and on the phosphorylation of PERK/eIF2α in the cortices of the tested mice by Western blotting. As indicated in Figure 9A, 9B, the protein level of sAPPβ/BACE1 and the phosphorylation of PERK/eIF2α in the transgenic mice were higher than those in the non-transgenic mice, whereas treatment with THA apparently inhibited those effects compared with the THA-non-treated transgenic group. Next, we carried out an RT-PCR assay to investigate if THA inhibits BACE1 transcription and found that THA failed to affect BACE1 mRNA levels (Figure 9C). These results indicated that THA alleviated PERK/eIF2α-mediated BACE1 translation in response to Aβ production inhibition in APP/PS1 transgenic mice, in line with the corresponding cell-based results.

THA stimulates both PI_3K/AKT/mTOR- and AMPK/Raptor/mTOR-mediated autophagy in APP/PS1 transgenic mice

Because THA has been determined to stimulate PI_3K/AKT/mTOR- and AMPK/Raptor/mTOR-mediated autophagy in the promotion of Aβ clearance in cells, we next inspected such effects in APP/PS1 transgenic mice. In the assay, we focused on the cortex of the tested mice by Western blotting.

THA stimulated autophagy

To examine the stimulation of THA against autophagy *in vivo*, we at first investigated the regulation of THA against the key proteins involved in the autophagy pathway. The results shown in Figure 9D, 9E revealed higher protein levels of p62 and phosphorylated ULK1 and lower protein levels of LC3II in vehicle-treated transgenic mice compared with those in vehicle-treated non-transgenic mice, which indicated the impaired autophagy process in transgenic mice[62]. Notably, THA administration obviously reversed all of these effects, thereby implying that THA could activate autophagy in APP/PS1 transgenic mice.

THA stimulated PI_3K/AKT/mTOR-mediated autophagy

Next, we examined the enhancement of THA on PI_3K/AKT/mTOR-mediated autophagy *in vivo*. As expected, Western blot results (Figure 9F–9I) indicated higher phosphorylation levels of PI_3K, AKT, mTOR and P70S6K in vehicle-treated transgenic mice compared with the levels in vehicle-treated non-transgenic mice. Indicative of the activated PI_3K/AKT/mTOR pathway in response to the impaired autophagy in APP/PS1 transgenic mice[41], administration of THA could obviously reverse all of the effects in the transgenic mice. These results thereby suggested that THA stimulated PI_3K/AKT/mTOR-mediated autophagy.

THA stimulated AMPK/Raptor/mTOR-mediated autophagy

Similarly, the Western blot results (Figure 9J, 9K) also indicated that administration of THA could activate the phosphorylation of AMPK/Raptor in APP/PS1 transgenic mice. Interestingly, the phosphorylation levels of AMPK and Raptor in the vehicle-treated transgenic mice were at similar levels as in non-transgenic mice.

Taken together, these results indicated that THA stimulated PI_3K/AKT/mTOR- and AMPK/Raptor/mTOR-mediated

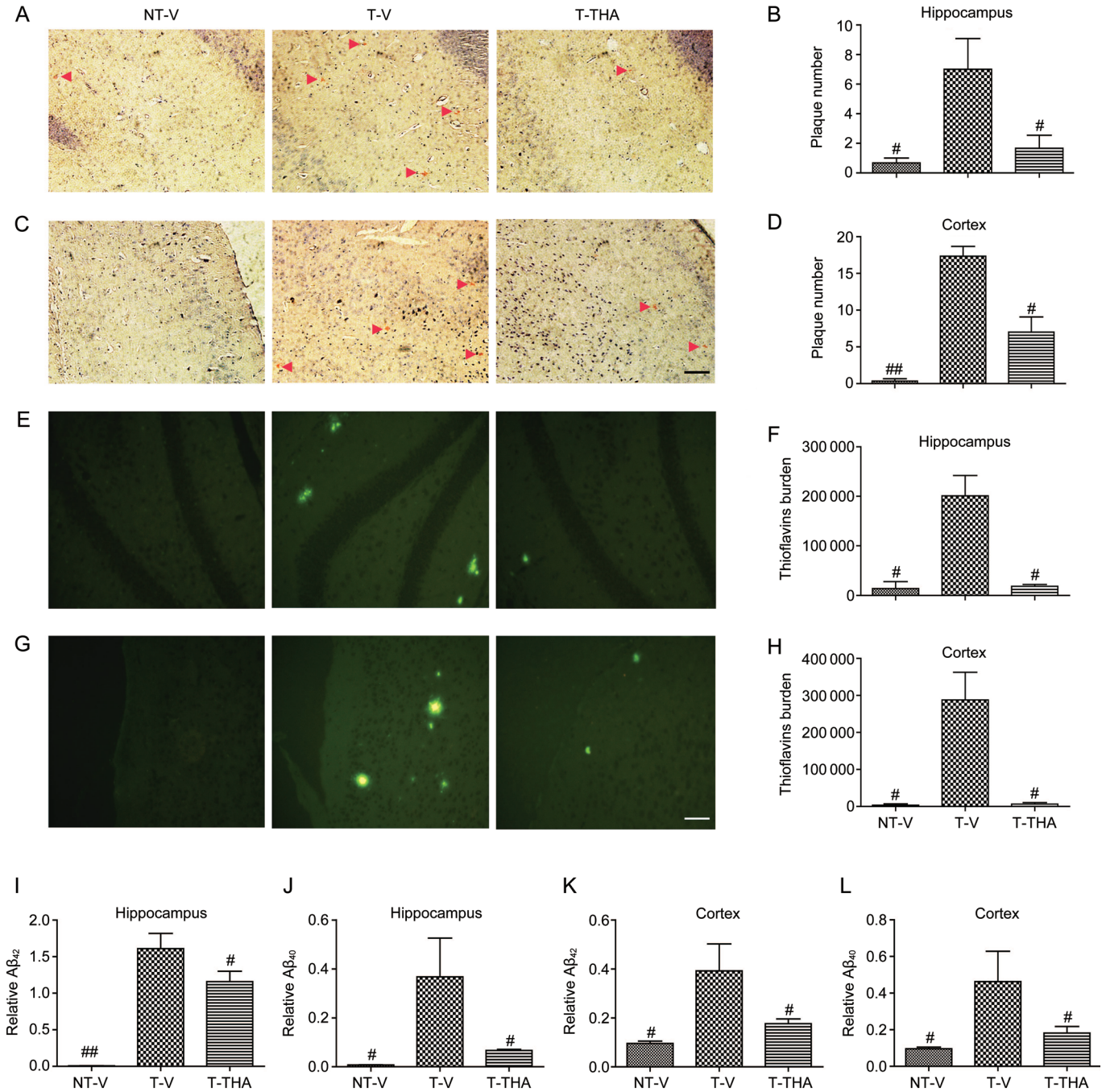

Figure 8. THA reduced senile plaques in the APP/PS1 transgenic mice. (A) An image of senile plaques stained with Congo red in the hippocampus. Red arrows indicate amyloid plaques. (B) Statistical analysis of image (A). (C) An image of senile plaques stained with Congo red in the cortex; the red arrows indicate amyloid plaques. (D) Statistical analysis of image (C). (E–H) An image of senile plaques stained with Thioflavine S in the hippocampus (E) and in the cortex (G). (F) Statistics of image (E). (H) Statistics of image (G). Scale bar, 100 μm. (I–L) An ELISA assay was used to evaluate the effect of THA on $A\beta_{40/42}$ levels in the APP/PS1 mice. NT-V, non-transgenic vehicle group; T-V, transgenic vehicle group; T-THA, transgenic mice administration with 300 mg THA/kg per day group. Values are the mean±SEM. *t* test. n=4. $^{\#}P<0.05$, $^{\#\#}P<0.01$ compared with T-V.

autophagy in APP/PS1 transgenic mice.

THA reduces Tau hyperphosphorylation involving inhibition of GSK3β in APP/PS1 transgenic mice

Given the published reports on the Tau-relevant study in APP/PS1 transgenic mice[34, 63], we also performed a Tau-related assay in the transgenic mice. In the assay, we investigated the potential of THA to inhibit Tau hyperphosphorylation *in vivo* by performing an immunohistochemical assay. As shown in Figure 10A–10D, Tau hyperphosphorylation bur-

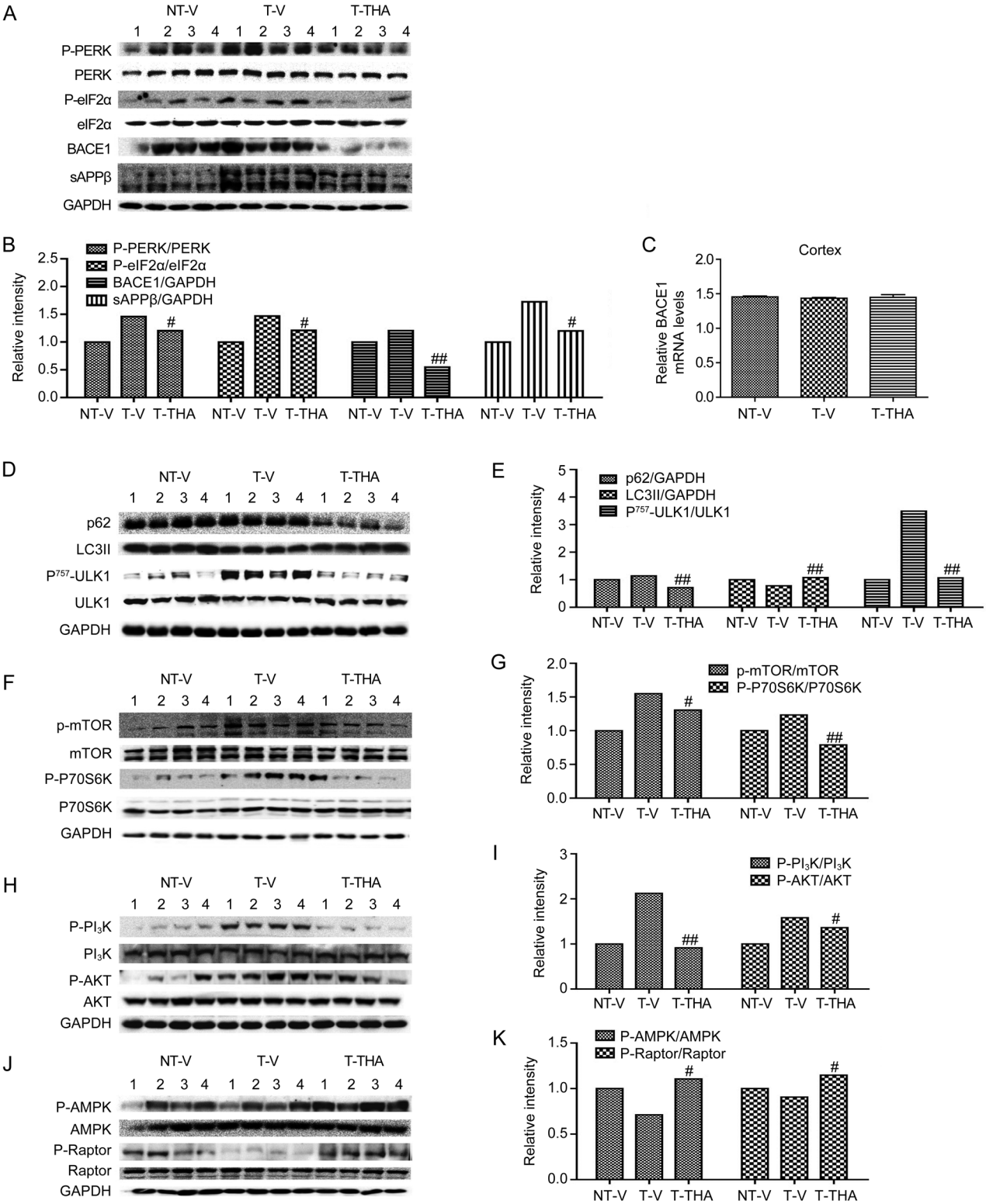

Figure 9. THA promoted Aβ clearance involving both PI_3K/AKT/mTOR and AMPK/Raptor/mTOR signaling-mediated autophagy activation. A Western blot assay was carried out for the cortices of the transgenic mice. (A) The levels of P-PERK, PERK, P-eIF2α, eIF2α, sAPPβ, and BACE1; (B) Densitometry analysis of (A). (C) BACE1 mRNA levels were detected by RT-PCR assays. (D) The levels of p62, LC3II, P-ULK1 and ULK1; (E) Densitometry analysis of (D); (F) The levels of P-mTOR, mTOR, P-P70S6K, and P70S6K; (G) Densitometry analysis of (F). (H) The levels of P-PI_3K, PI_3K, P-AKT, and AKT; (I) Densitometry analysis of (H). (J) The levels of P-AMPK, AMPK, P-Raptor and Raptor; (K) Densitometry analysis of (J); GAPDH was used as a loading control in the Western blot assays. NT-V, non-transgenic vehicle group; T-V, transgenic vehicle group; T-THA, transgenic mice administration with 300 mg THA/kg per day group. Values are the mean±SEM. *t* test. n=4. $^{\#}P<0.05$, $^{\#\#}P<0.01$ compared with T-V.

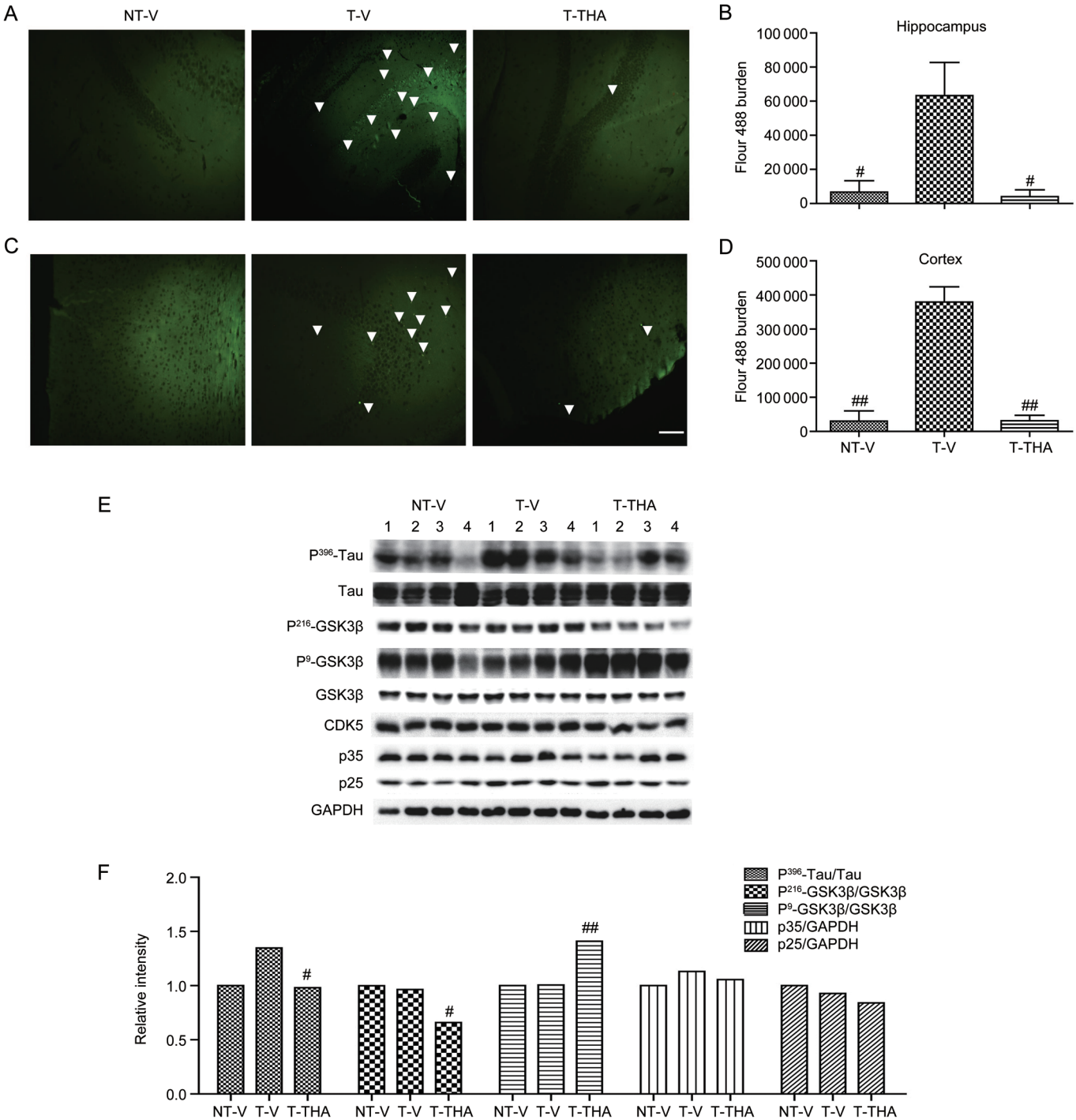

Figure 10. THA reduced Tau phosphorylation by inhibiting GSK3β activity in the APP/PS1 transgenic mice. (A–D) Immunohistochemical assay was performed to detect the Tau phosphorylation burden in the hippocampus (A) and cortex (C); white arrows indicate Tau phosphorylation. (B) Statistical analysis of (A). (D) Statistical analysis of (C). Scale bar, 100 μm. (E) The levels of Tau at Serine396, GSK-3β (phosphorylated at Ser9 or Tyr216), GSK-3β, CDK5 and p35/p25 were tested by Western blot. (F) Densitometry analysis of (E). GAPDH was used as a loading control in the Western blot assays. NT-V, non-transgenic vehicle group; T-V, transgenic vehicle group; T-THA, transgenic mice administration with 300 mg THA/kg per day group. Values are the mean±SEM. *t* test. $^{\#}P<0.05$, $^{\#\#}P<0.01$ compared with T-V.

dens in the hippocampus and cortex of vehicle-administered transgenic mice were more severe than in the vehicle-administered non-transgenic mice group, and THA administration effectively reversed these effects in the transgenic mice.

Subsequently, a Western blot assay was performed. Similar to the cell-based assays, we investigated the effects of THA on

GSK3β phosphorylation at Ser9/Tyr216 and CDK5 and p35/p25 protein levels in the transgenic mice. As shown in Figure 10E, 10F, an approximately 40% change in p-Tau/Tau between wild-type and AD mice was determined, and this result was close to a published report where a 50% change in p-Tau/Tau between wild-type and AD mice was found[64, 65]. In addition, THA administration stimulated the inactive form of GSK3β (phosphorylated at Ser9) and inhibited the active form of GSK3β (phosphorylated at Tyr216) in APP/PS1 transgenic mice, indicating that THA could inhibit GSK3β activity *in vivo*. As expected, THA had no effects on CDK5 or p35/p25 in the mice (Figure 10E, 10F). Thus, the results demonstrated that THA reduced Tau phosphorylation by inhibition of GSK3β in the APP/PS1 transgenic mice, in consistence with the cell-based results.

THA prolongs the lifespan of wild-type *Drosophila melanogaster*

Accumulating evidence has revealed that aging is highly associated with AD, and delaying aging is an applicable strategy for decreasing AD rates and postponing AD progression[66], while autophagy is tightly linked to lifespan[67]. Given these facts, we thus investigated the potential of THA to extend the lifespan of *Drosophila melanogaster*. As expected, the results indicated that THA treatment (0.05 mg/mL) effectively extended the lifespan of *Drosophila melanogaster* (Figure 11). This result thereby supported that THA may prevent AD by delaying aging.

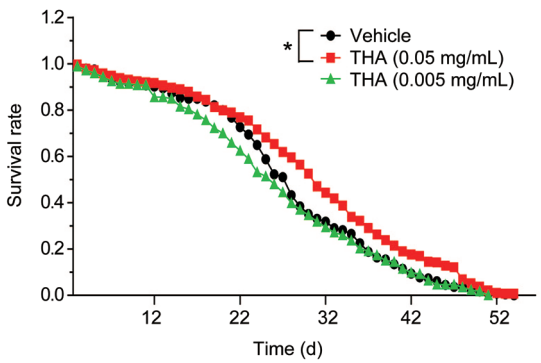

Figure 11. THA treatment extended the lifespan of wild-type *Drosophila melanogaster*. THA treatment extended the lifespan of *Drosophila melanogaster*. Lifespans of vehicle- and THA-treated *Drosophila melanogaster* were analyzed according to increases in the median lifespans. Kaplan-Meier, log-rank test, Mantel Cox, $^{*}P<0.05$, compared with the vehicle group, Vehicle group: 0 mg/LTHA treatment group.

Discussion

Along with the fast pace of an aging society are aging diseases (*eg*, AD, type 2 diabetes, cancers, *etc*), which severely afflict the aged population. In fact, the neurodegenerative disease AD has been clinically accepted as one of the leading causes of death[24]. It is characterized by progressive memory loss and cognitive and behavioral disturbances, and there is no efficient treatment against this disease, although there have been clinical drugs capable of improving the symptoms of AD[68]. Considering the complicated pathogenesis of AD, multi-targets have become a focus in the discovery of drug compounds for treatment of this disease[18]. In the current work, given the diversities in both the chemical structures and acting targets for natural products, we established a multi-target strategy for discovering active reagents capable of suppressing both Aβ levels and Tau hyperphosphorylation from natural products. We found that the extract of *Thamnolia vermicularis* improves learning ability in APP/PS1 transgenic mice by ameliorating both Aβ and Tau pathologies, which highly supports the efficiency of our strategy for the discovery of potential anti-AD agents.

Recently, several pharmacological functions have been discovered for the lichen *Thamnolia vermicularis* in the treatment of various diseases, including hypertension, cough, and neurasthenia, and for its antioxidant and anticancer properties[20, 22]. Therefore, our current results concerning its anti-AD activity have also expanded the new pharmacological functions for this natural product. Various types of pure small molecules have been separated from *Thamnolia vermicularis*[69], but no report has yet been published regarding their potential multi-target function in the treatment of AD. Considering the relatively high contents of squamatic acid (42%) and baeomycesic acid (46%) (Figure 1A) in THA, we also examined the potential activity of these two compounds in the regulation of Aβ accumulation and/or Tau phosphorylation, and the results indicated that neither of these two compounds exhibited effects (data not shown). Currently, few reports have been published on the functions of baeomycesic acid and squamatic acid[70, 71], and baeomycesic acid was determined to exhibit antiproliferative effects on several human tumor cell lines[72]. Thus, it is expected that the current study may also provide chemical direction for the discovery of compounds with multi-target activities in the repression of Aβ/Tau pathology from *Thamnolia vermicularis*.

In summary, we reported that the ethanol extract of *Thamnolia vermicularis* (THA) improved learning ability in APP/PS1 transgenic mice by inhibiting both Aβ levels and Tau hyperphosphorylation. In addition, THA as an effective autophagy activator, also efficiently prolonged the lifespan of wild-type *Drosophila melanogaster*, thus exhibiting potential in the prevention of AD by prolonging aging. Figure 12 shows a proposed model for the amelioration of Aβ/Tau pathology by THA. THA stimulated either PI_3K/AKT/mTOR- or AMPK/raptor/mTOR signaling-mediated autophagy in promotion of Aβ clearance as both a PI_3K inhibitor and an AMPK indirect activator and restrained Aβ production as a suppressor against PERK/eIF2α-mediated BACE1 expression. Additionally, as a GSK3β inhibitor, THA inhibited Tau hyperphosphorylation. Therefore, our results have highlighted the potential of THA in the treatment of AD.

Acknowledgements

This work was supported by the National Natural Sci-

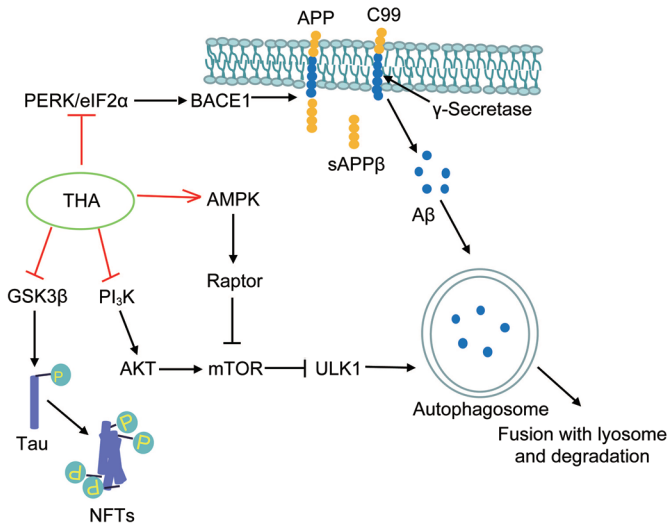

Figure 12. A proposed model showing the amelioration of THA on Aβ/Tau pathology. Senile plaques formed by Aβ deposition and NFTs composed of hyperphosphorylated Tau are believed to be two major hallmarks of AD pathology. THA stimulated either PI_3K/AKT/mTOR- or AMPK/raptor/mTOR signaling-mediated autophagy in promoting Aβ clearance as both a PI_3K inhibitor and an AMPK indirect activator. THA restricted Aβ production as a suppressor against PERK/eIF2α-mediated BACE1 expression. Additionally, THA functioned as a GSK3β inhibitor, repressing Tau hyperphosphorylation.

ence Foundation of China (81220108025, 81473141, and 81273556), NSFC-TRF collaboration projects (81561148011 and DBG5980001) and the Drug Innovation Project of SIMM (CASIMM0120154035). The authors are grateful to JoeKai company (Suzhou, China) for the assay of the lifespan of wild-type *Drosophila melanogaster*.

Author contribution

Xu SHEN, Zhi-yuan ZHU, and Cong LI designed the study; Cong LI carried out the experiments and analyzed the data; Min LEI and Li-hong HU synthesized the compound; Zhi-yuan ZHU, Xiao-fan SHI, and Xiao-dan GUO participated in animal experiments; Xu SHEN and Cong LI wrote the manuscript; all authors, including Tie-qiao WEN, Jia-yi WU, Jia-zhen JIN, and Vatcharin RUKACHAISIRIKUL, discussed the results and contributed to the revision of the final manuscript.

Supplementary information

Supplementary figures are available on the website of Acta Pharmacologica Sinica.

References

1 Hardy J. A hundred years of Alzheimer's disease research. Neuron 2006; 52: 3–13.
2 Walsh DM, Selkoe DJ. Deciphering the molecular basis of memory failure in Alzheimer's disease. Neuron 2004; 44: 181–93.
3 Vassar R, Bennett BD, Babu-Khan S, Kahn S, Mendiaz EA, Denis P, *et al.* beta-secretase cleavage of Alzheimer's amyloid precursor protein by the transmembrane aspartic protease BACE. Science 1999; 286: 735–41.
4 Ghosh AK, Osswald HL. BACE1 (beta-secretase) inhibitors for the treatment of Alzheimer's disease. Chem Soc Rev 2014; 43: 6765–813.
5 Yi H, Lee SJ, Lee J, Myung CS, Park WK, Lim HJ, *et al.* Sphingosylphosphorylcholine attenuated beta-amyloid production by reducing BACE1 expression and catalysis in PC12 cells. Neurochem Res 2011; 36: 2083–90.
6 Rossner S, Sastre M, Bourne K, Lichtenthaler SF. Transcriptional and translational regulation of BACE1 expression — Implications for Alzheimer's disease. Prog Neurobiol 2006; 79: 95–111.
7 Ghosh AK, Brindisi M, Tang J. Developing β-secretase inhibitors for treatment of Alzheimer's disease. J Neurochem 2012; 120: 71–83.
8 Abdel-Magid AF. beta-Secretase inhibitors for the treatment of Alzheimer's disease and down's syndrome. ACS Med Chem Lett 2013; 4: 13–4.
9 Jakob-Roetne R, Jacobsen H. Alzheimer's disease: from pathology to therapeutic approaches. Angew Chem Int Ed Enql 2009; 48: 3030–59.
10 Klionsky DJ, Emr SD. Cell biology — autophagy as a regulated pathway of cellular degradation. Science 2000; 290: 1717–21.
11 Chan EYW, Longatti A, McKnight NC, Tooze SA. Kinase-inactivated ULK proteins inhibit autophagy via their conserved C-terminal domains using an Atg13-independent mechanism. Mol Cell Biol 2009; 29: 157–71.
12 Franke TF, Kaplan DR, Cantley LC, Toker A. Direct regulation of the Akt proto-oncogene product by phosphatidylinositol-3,4-bisphosphate. Science 1997; 275: 665–8.
13 Singh TJ, Grundkeiqbal I, Mcdonald B, Iqbal K. Comparison of the phosphorylation of microtubule-associated protein-Tau by non-proline dependent protein-kinases. Mol Cell Biochem 1994; 131: 181–9.
14 Wang JZ, Wu QL, Smith A, Grundke-Iqbal I, Iqbal K. Tau is phosphorylated by GSK-3 at several sites found in Alzheimer disease and its biological activity markedly inhibited only after it is prephosphorylated by A-kinase. FEBS Lett 1998; 436: 28–34.
15 Kimura T, Ishiguro K, Hisanaga SI. Physiological and pathological phosphorylation of tau by Cdk5. Front Mol Neurosci 2014; 7: 65.
16 Fan LY, Chiu MJ. Combotherapy and current concepts as well as future strategies for the treatment of Alzheimer's disease. Neuropsych Dis Treat 2014; 10: 439–51.
17 Doody RS. Phase 3 trials of solanezumab for mild-to-moderate Alzheimer's disease. N Engl J Med 2014; 370: 311–21.
18 Zheng H, Fridkin M, Youdim M. New approaches to treating Alzheimer's disease. Perspect Medicin Chem 2015; 7: 1–8.
19 Kalra J, Khan A. Reducing A beta load and tau phosphorylation: Emerging perspective for treating Alzheimer's disease. Eur J Pharmacol 2015; 764: 571–81.
20 Luo H, Ren M, Lim KM, Koh YJ, Wang LS, Hur JS. Antioxidative activity of lichen *Thamnolia vermicularis in vitro*. Mycobiology 2006; 34: 124–7.
21 Wang LS, Narui T, Harada H, Culberson CF, Culberson WL. Ethnic uses of lichens in Yunnan, China. Bryologist 2001; 104: 345–9.
22 Marijana K, Branislav R. Antibacterial and antifungal activity of different lichens extracts and lichen acid. Res J Biotechnol 2011; 6: 23–6.
23 Guo J, Li ZL, Wang AL, Liu XQ, Wang J, Guo X, *et al.* Three new phenolic compounds from the lichen *Thamnolia vermicularis* and their antiproliferative effects in prostate cancer cells. Planta Med 2011; 77: 2042–6.
24 Xiang WJ, Wang QQ, Ma L, Hu LH. Orcinol-type depsides from the lichen *Thamnolia vermicularis*. Nat Prod Res 2013; 27: 804–8.

25 Paresce DM, Chung HY, Maxfield FR. Slow degradation of aggregates of the Alzheimer's disease amyloid beta-protein by microglial cells. J Biol Chem 1997; 272: 29390–7.
26 Ard MD, Cole GM, Wei J, Mehrle AP, Fratkin JD. Scavenging of Alzheimer's amyloid beta-protein by microglia in culture. J Neurosci Res 1996; 43: 190–202.
27 Shaffer LM, Dority MD, Guptabansal R, Frederickson RCA, Younkin SG, Brunden KR. Amyloid-beta protein (a-beta) removal by neuroglial cells in culture. Neurobiol Aging 1995; 16: 737–45.
28 Zhang H, Gao Y, Zhao FL, Qiao PF, Yan Y. Hydrogen sulfide-induced processing of the amyloid precursor protein in SH-SY5Y human neuroblastoma cells involves the PI3-K/Akt signaling pathway. Cell Mol Neurobiol 2015; 35: 265–72.
29 Kovalevich J, Langford D. Considerations for the use of SH-SY5Y neuroblastoma cells in neurobiology. Methods Mol Biol 2013; 1078: 9–21.
30 Busciglio J, Gabuzda DH, Matsudaira P, Yankner BA. Generation of beta-amyloid in the secretory pathway in neuronal and nonneuronal cells. Proc Natl Acad Sci U S A 1993; 90: 2092–6.
31 Guenette SY. Mechanisms of A beta clearance and catabolism. Neuromol Med 2003; 4: 147–60.
32 Groemer TW, Thiel CS, Holt M, Riedel D, Hua YF, Huve J, *et al.* Amyloid precursor protein is trafficked and secreted via synaptic vesicles. PLoS One 2011; 6: e18754.
33 Bhat R, Crowe EP, Bitto A, Moh M, Katsetos CD, Garcia FU, *et al.* Astrocyte senescence as a component of Alzheimer's disease. PLoS One 2012; 7: e45069.
34 Tanaka T, Iqbal K, Trenkner E, Liu DJ, Grundkeiqbal I. Abnormally phosphorylated-Tau in Sy5y human neuroblastoma-cells. FEBS Lett 1995; 360: 5–9.
35 Wojcikiewicz RJ, Tobin AB, Nahorski SR. Muscarinic receptor-mediated inositol 1,4,5-trisphosphate formation in SH-SY5Y neuroblastoma cells is regulated acutely by cytosolic Ca^{2+} and by rapid desensitization. J Neurochem 1994; 63: 177–85.
36 Feany MB, Dickson DW. Widespread cytoskeletal pathology characterizes corticobasal degeneration. Am J Pathol 1995; 146: 1388–96.
37 Shin RW, Iwaki T, Kitamoto T, Tateishi J. Methods in laboratory investigation — hydrated autoclave pretreatment enhances Tau immunoreactivity in formalin-fixed normal and Alzheimers-disease brain-tissues. Lab Invest 1991; 64: 693–702.
38 Cramer PE, Cirrito JR, Wesson DW, Lee CYD, Karlo JC, Zinn AE, *et al.* ApoE-directed therapeutics rapidly clear beta-amyloid and reverse deficits in AD mouse models. Science 2012; 335: 1503–6.
39 Jiang Q, Lee CY, Mandrekar S, Wilkinson B, Cramer P, Zelcer N, *et al.* ApoE promotes the proteolytic degradation of Abeta. Neuron 2008; 58: 681–93.
40 Zhu ZY, Li CJ, Wang X, Yang ZY, Chen J, Hu LH, *et al.* 2,2′,4′-Trihydroxychalcone from *Glycyrrhiza glabra* as a new specific BACE1 inhibitor efficiently ameliorates memory impairment in mice. J Neurochem 2010; 114: 374–85.
41 Brasca MG, Albanese C, Alzani R, Amici R, Avanzi N, Ballinari D, *et al.* Optimization of 6,6-dimethyl pyrrolo[3,4-c]pyrazoles: Identification of PHA-793887, a potent CDK inhibitor suitable for intravenous dosing. Bioorgan Med Chem 2010; 18: 1844–53.
42 Raught B, Gingras AC, Sonenberg N. The target of rapamycin (TOR) proteins. Proc Natl Acad Sci U S A 2001; 98: 7037–44.
43 Zhu ZY, Yan JM, Jiang W, Yao XG, Chen J, Chen LL, *et al.* Arctigenin effectively ameliorates memory impairment in Alzheimer's disease model mice targeting both beta-amyloid production and clearance. J Neurosci 2013; 33: 13138–49.
44 Zhang YW, Thompson R, Zhang H, Xu HX. APP processing in Alzheimer's disease. Mol Brain 2011; 4.
45 O'Connor T, Sadleir KR, Maus E, Velliquette RA, Zhao J, Cole SL, *et al.* Phosphorylation of the translation initiation factor eIF2alpha increases BACE1 levels and promotes amyloidogenesis. Neuron 2008; 60: 988–1009.
46 Himes RA, Park GY, Barry AN, Blackburn NJ, Karlin KD. Synthesis and X-ray absorption spectroscopy structural studies of Cu(I) complexes of HistidylHistidine peptides: The predominance of linear 2-coordinate geometry. J Am Chem Soc 2007; 129: 5352–3.
47 Raffa DF, Rickard GA, Rauk A. Ab initio modelling of the structure and redox behaviour of copper(I) bound to a His-His model peptide: relevance to the beta-amyloid peptide of Alzheimer's disease. J Biol Inorg Chem 2007; 12: 147–64.
48 Sarell CJ, Wilkinson SR, Viles JH. Substoichiometric levels of Cu^{2+} ions accelerate the kinetics of fiber formation and promote cell toxicity of amyloid-beta from Alzheimer disease. J Biol Chem 2010; 285: 41533–40.
49 Rubinsztein DC, Gestwicki JE, Murphy LO, Klionsky DJ. Potential therapeutic applications of autophagy. Nat Rev Drug Discov 2007; 6: 304–12.
50 Xu B, Bai B, Sha SM, Yu PF, An YX, Wang SQ, *et al.* Interleukin-1 beta induces autophagy by affecting calcium homeostasis and trypsinogen activation in pancreatic acinar cells. Int J Clin Exp Patho 2014; 7: 3620–31.
51 Xu XY, Fu YX, Tong J, Fan SX, Xu K, Sun H, *et al.* MicroRNA-216b/Beclin 1 axis regulates autophagy and apoptosis in human Tenon's capsule fibroblasts upon hydroxycamptothecin exposure. Exp Eye Res 2014; 123: 43–55.
52 He CC, Klionsky DJ. Regulation mechanisms and signaling pathways of autophagy. Annu Rev Genet 2009; 43: 67–93.
53 Kimura T, Takabatake Y, Takahashi A, Isaka Y. Chloroquine in cancer therapy: a double-edged sword of autophagy. Cancer Res 2013; 73: 3–7.
54 Chan EYW, Kir S, Tooze SA. SiRNA screening of the kinome identifies ULK1 as a multidomain modulator of autophagy. J Biol Chem 2007; 282: 25464–74.
55 Arcaro A, Wymann MP. Wortmannin Is a potent phosphatidylinositol 3-kinase inhibitor — the role of phosphatidylinositol 3,4,5-trisphosphate in neutrophil responses. Biochem J 1993; 296: 297–301.
56 Cool B, Zinker B, Chiou W, Kifle L, Cao N, Perham M, *et al.* Identification and characterization of a small molecule AMPK activator that treats key components of type 2 diabetes and the metabolic syndrome. Cell Metab 2006; 3: 403–16.
57 Cheng D, Logge W, Low JK, Garner B, Karl T. Novel behavioural characteristics of the APP_{Swe}/PS1ΔE9 transgenic mouse model of Alzheimer's disease. Behav Brain Res 2013; 245: 120–7.
58 Bromley-Brits K, Deng Y, Song W. Morris water maze test for learning and memory deficits in Alzheimer's disease model mice. J Vis Exp 2011; (53): 2920.
59 Hardy J. Amyloid, the presenilins and Alzheimer's disease. Trends Neurosci 1997; 20: 154–9.
60 Lei Y, Yang L, Ye CY, Qin MY, Yang HY, Jiang HL, *et al.* Involvement of intracellular and mitochondrial Aβ in the ameliorative effects of huperzine A against oligomeric $Aβ_{42}$-induced injury in primary rat neurons. PLoS One 2015; 10: e0128366.
61 Yang L, Ye CY, Huang XT, Tang XC, Zhang HY. Decreased accumulation of subcellular amyloid-beta with improved mitochondrial function mediates the neuroprotective effect of huperzine A. J Alzheimers Dis 2012; 31: 131–42.
62 Orr ME, Oddo S. Autophagic/lysosomal dysfunction in Alzheimer's

disease. Alzheimers Res Ther 2013; 5.
63 Wojcikiewicz RJ, Tobin AB, Nahorski SR. Muscarinic receptor-mediated inositol 1,4,5-trisphosphate formation in Sh-Sy5y neuroblastoma-cells Is regulated acutely by cytosolic Ca^{2+} and by rapid desensitization. J Neurochem 1994; 63: 177–85.
64 Ramos-Rodriguez JJ, Molina-Gil S, Rey-Brea R, Berrocoso E, Garcia-Alloza M. Specific serotonergic denervation affects tau pathology and cognition without altering senile plaques deposition in APP/PS1 mice. PLoS One 2013; 8: e79947.
65 Fang YQ, Yao LM, Li CH, Wang J, Wang JN, Chen SJ, *et al*. The blockage of the Nogo/NgR signal pathway in microglia alleviates the formation of A beta plaques and tau phosphorylation in APP/PS1 transgenic mice. J Neuroinflamm 2016; 13: 56.
66 Jirillo E, Candore G, Magrone T, Caruso C. A scientific approach to anti-ageing therapies: state of the art. Curr Pharm Design 2008; 14: 2637–42.
67 He LQ, Lu JH, Yue ZY. Autophagy in ageing and ageing-associated diseases. Acta Pharmacol Sin 2013; 34: 605–11.
68 Salloway S, Sperling R, Fox NC, Blennow K, Klunk W, Raskind M, *et al*. Two phase 3 trials of bapineuzumab in mild-to-moderate Alzheimer's disease. N Engl J Med 2014; 370: 322–33.
69 Jiang B, Mei SX, Han QB, Xiang W, Sun HD. A new phenolic compound from *Thamnolia vermicularis*. Chin Chem Lett 2001; 12: 47–8.
70 Molnar K, Farkas E. Current results on biological activities of lichen secondary metabolites: a review. Z Naturforsch C 2010; 65: 157–73.
71 Zambare VP, Christopher LP. Biopharmaceutical potential of lichens. Pharm Biol 2012; 50: 778–98.
72 Haraldsdottir S, Gudlaugsdottir E, Ingolfsdottir K, Ogmundsdottir HM. Anti-proliferative effects of lichen-derived lipoxygenase inhibitors on twelve human cancer cell lines of different tissue origin *in vitro*. Planta Med 2004; 70: 1098–100.